Title

The Metabolism and Toxicity of Radium-223 in Rats

Authors

Durbin, Patricia W
Asling, C Willet
Jeung, Nylan
et al.

Publication Date

1958-02-01

UCRL 8189

UNIVERSITY OF
CALIFORNIA

Radiation Laboratory

THE METABOLISM AND TOXICITY OF RADIUM-223 IN RATS

DISCLAIMER

UCRL-8189
Health and Biology

UNIVERSITY OF CALIFORNIA
Radiation Laboratory
Berkeley, California

Contract No. W-7405-eng-48

THE METABOLISM AND TOXICITY OF RADIUM-223 IN RATS

Patricia W. Durbin, C. Willet Asling, Nylan Jeung,
Marilyn H. Williams, James Post, Muriel E. Johnston, and
Joseph G. Hamilton

February 21, 1958

Printed for the U. S. Atomic Energy Commission

THE METABOLISM AND TOXICITY OF RADIUM-223 IN RATS

Patricia W. Durbin, C. Willet Asling, Nylan Jeung, Marilyn H. Williams, James Post, Muriel E. Johnston, and Joseph G. Hamilton

Crocker Laboratory and Division of Medical Physics
and Department of Anatomy
University of California, Berkeley, California

February 21, 1958

ABSTRACT

This report covers studies of the excretion and retention of "tracer" and toxic doses of the 11.2-day Ra^{223} isotope, its acute toxicity (organ weight changes, gross and microscopic pathology, and Fe^{59} utilization by the bone marrow), and long-term histopathological changes and alterations in the hemogram.

Young adult female Sprague-Dawley rats (110 days old) were used. Ra^{223} was injected intramuscularly in sodium citrate at dosages ranging from 0.0004 to 0.10 μC/g body weight. The animals reserved for long-term study were followed for Ra^{223} retention for the first 60 days, and complete blood counts were performed on these animals periodically. A second group under study for acute changes received Fe^{59} on the fifth day and were sacrificed on the eighth day after the Ra^{223} injection. Blood counts were taken, Fe^{59} uptake was determined by standard techniques, and tissues were weighed and prepared for histological study. Radiation dosages to the skeleton and bone marrow were estimated from skeletal retention curves.

Excretion and retention curves are presented. Both elimination and retention were influenced by the Ra^{223} dosage. At high Ra^{223} dosages total excretion followed a power function with a slope $T^{-1.5}$; at the lowest Ra^{223} level excretion was more nearly described by a series of exponentials. The relationship between the type of excretion curve obtained and the extent of skeletal radiation damage is discussed.

Ra^{223} proved to be highly toxic, and to have a 30-day mean lethal dose of about 0.05 μC/g body weight. In the acutely lethal range there were significant body weight losses and tissue wasting, particularly noticeable in the lymph nodes of the G-I tract, and in the spleen and thymus. Microscopically these tissues showed cell depletion rather than destruction. Hemorrhage was believed to be the most probable cause of death in those animals that succumbed during the first 30 days.

Curves relating marrow status (red cell Fe^{59} uptake and granulocyte count) to increasing Ra^{223} dose were complex and showed steep initial components that were attributed to direct cellular destruction. The processes responsible for the less radiation-sensitive components are discussed, particularly general nutritional impairment and skeletal vascular damage.

The notable reduction of the lymphocyte count without demonstrable radiation damage in the soft tissues is discussed in the light of the normal presence of large numbers of adult lymphocytes in the bone marrow of rodents.

Effects of Ra^{223} on bone growth were studied in the distal epiphysis of the femur, which is still growing slowly in rats of this age. At the lowest dosage, 0.004 μC/g, changes observed in specimens taken 8 days after the Ra^{223} injection consisted of death of some cartilage cells, reduction in the number of capillary tufts impinging on the cartilage plate, and reduction in the number of osteoblasts. At dosages near the acutely lethal level proliferation of the epiphyseal cartilage was in abeyance, the marrow immediately below the plate was avascular, osteoblasts were rare, and osteoclastic activity was much reduced. Specimens taken from animals receiving lethal amounts of Ra^{223} showed all of the above changes to a high degree, and in addition, the mechanism whereby cartilage is normally calcified was apparently lost.

Even at the lowest Ra^{223} dosages, bone growth did not resume to any measurable extent, and the epiphysis was sealed off from the marrow cavity by bone. The mechanism responsible for bone resorption was apparently less deranged, so that by the 500th day, the old spongiosa in the metaphysis had been almost completely removed. The bones from the higher-level animals taken at 200 days reflected their greater initial injury in a reduced ability of the capillaries to grow back into the heavily irradiated regions, in a marked reduction in capacity for bone remodeling and resorption, and--at the very highest Ra^{223} dosages for which there were long-term survivors--in failure to calcify pre-existing cartilage.

A large discrepancy was noted between the 30-day mean lethal dose of natural radium, Ra^{226}, determined for mice and rats of another strain (1.0 μC/g body weight), and the lethal dosage that would be expected from this isotope and its radioactive daughters based on calculations from our experiments with Ra^{223}. This discrepancy can be explained in part by differences in the rate of radiation dose delivery and the varying ability of the animals under study to engage in splenic ectopic myelopoiesis.

THE METABOLISM AND TOXICITY OF RADIUM-223 IN RATS

Patricia W. Durbin, C. Willet Asling, Nylan Jeung, Marilyn H. Williams, James Post, Muriel E. Johnston, and Joseph G. Hamilton

Crocker Laboratory and Division of Medical Physics
and Department of Anatomy
University of California, Berkeley, California

February 21, 1958

INTRODUCTION

Campbell et al. have demonstrated metabolic patterns for thorium-227 and radium-223 that are independent of the metabolism of their parent isotope actinium-227.[1] These investigators indicated that the independent behavior would profoundly influence the potential hazard associated with the actinium series. They further showed that the toxic action of an Ac^{227} equilibrium mixture (AEM) following oral adminstration or intramuscular injection (in the absence of a complexing agent) or transfer from actinium-bearing mothers to their nurslings, was chiefly due to the Ra^{223}.[1] In the chain decay of Ac^{227} to Pb^{207}--the natural 4n+3 radioactive series--82% of the total available energy is derived from the 11.2-day Ra^{223} and its three alpha-emitting daughters.[2] It was therefore of interest to study the metabolism and toxicity of Ra^{223} when separated from its parents, Ac^{227} and Th^{227}.

In addition, this isotope of radium possesses certain advantages in the investigation of radium toxicity and metabolism per se: (a) the half life of the radon isotope in the series, Rn^{219}, is sufficiently short (3.9 sec) so that one can assume that its release from the skeleton is negligible; and (b) metabolic studies can be conducted for as long as 2 months afterwards by injection of as little as 2×10^{-5} microgram (1μC) of Ra^{223}, with a total radiation dosage to the skeleton of about one-half that delivered by 1 microgram of Ra^{226} (1μC).

Apart from the interest in this isotope as a potential health hazard in conjunction with the other members of the actinium series, Ra^{223} is also valuable in radiobiological studies. Because of its short half life, intense alpha radiation can be delivered to the skeleton and bone marrow during a short interval of time, and survivors can then be observed for recovery and (or) reparative changes without the usual complications of continuous irradiation.

This report covers studies of the excretion and distribution of "tracer" and toxic doses of Ra^{223} during the first 60 days after administration, the acute toxicity of Ra^{223} (organ-weight changes, gross and microscopic pathology, and Fe^{59} utilization), long-term histopathological changes, and alterations in the levels of the cellular elements of the blood.

METHODS

The animals used in these studies were young adult female Sprague-Dawley rats 90 to 115 days of age obtained from the original colony. They were housed in metal cages on wood shavings in groups of five, and were fed Purina Laboratory Chow and tap water ad lib. Respiratory infections were controlled by administering aureomycin (unrefined, Lederle) at a level of 2.5 g per pint of drinking water for two days every other week. One week before radioisotope injection the animals were distributed at random into groups of 20. Pre-injection red cell count, hemoglobin, microhematocrit, white cell count, and differential white count were measured in tail blood.

A stock solution of AEM was placed on a 2-cm column of Dowex-50 ion-exchange resin, and the Ra^{223} was separated by elution with 2 N HNO_3. The Ra^{223} solutions were prepared for injection by dilution with a 30-mg/ml solution of sodium citrate, so that the desired dosage was contained in a volume of 0.1 to 0.5 ml. The dosage for each group of rats was based upon the mean body weight of the group, and the volume administered was varied for those animals whose body weights differed by more than 10% from the mean for the group. Intramuscular injections were made into the left hind leg without anaesthesia. Twenty rats were injected at each of these dosage levels: 0.004 μC/g, 0.02μC/g, 0.04 μC/g, 0.07 μC/g, and 0.10 μC/g. In addition, 10 rats each received Ra^{223} at levels of 0.0004 μC/g, 0.001 μC/g, 0.002 μC/g, 0.003 μC/g, and 0.008 μC/g. Twenty uninjected rats served as controls. Half the animals at the five higher dosages and half the control animals comprised Group A and were used for the study of Ra^{223} retention, long-term alterations in the formed blood elements, and shortening of life span. The remaining half of the high-level Ra^{223} rats, the five lower-level groups, and 10 controls constituted Group B and were used to study the acute effects of Ra^{223} alpha irradiation. Tracer studies were performed on 15 rats that were given intramuscular injections of 1.5 μC of Ra^{223} in isotonic saline. These animals were placed in metabolism cages in groups of two or three; urine and feces were collected separately. Groups of five rats were sacrificed 1, 8, and 16 days after injection. Various soft tissues and bones were dissected, weighted, ashed, and prepared for radioactive assay.

After injection the rats in Group A were placed in metabolism cages in lots of five per cage. The cages were checked daily for dead rats. When a death occurred, excreta from that cage were pooled; otherwise, excreta were collected on alternate days. The accuracy of the assay of the Ra^{223} in the excreta was checked by measuring the residual radioactivity in the dead animals. By the 60th day radioactive decay and the decline in excretion rate made it difficult to assay the excreta with an accuracy of better than ± 15%. Excretion collections were discontinued, and the surviving animals were returned to stock cages.

All Group A survivors were weighted and complete blood counts were taken weekly for the first 4 weeks, then biweekly until the 30th week, and monthly thereafter. Alterations in the sizes of the red blood cells were determined from measurements with a camera lucida and ruled paper on 40 randomly selected cells on each dried smear.

The rats in Group A that survived the acute radiation period were allowed to live out the remainder of their life span. Animals that demonstrated a precipitous weight loss during a 2- to 4-week period were presumed to be very near death and were sacrificed. At autopsy, samples were taken of spleen, lymph nodes, thymus, liver, femur, vertebrae, rib, and mandible. The tissue specimens were fixed in Zenker-formol. The bones were decalcified. Tissues were mounted in paraffin and stained with Harris's hematoxylin and azure eosin, Jenner-Giemsa, or hematoxylin and eosin.

On the fifth day after tha Ra^{223} adminstration the Group B rats each received 2.5 μC of high-specific-activity Fe^{59} as $FeCl_3$ intravenously. On the eighth day after the Ra^{223} injection (third day after Fe^{59}), they were anesthetized with ether and a 5-ml blood sample was withdrawn from the inferior vena cava. A small portion of the mixed venous blood was utilized for duplicate determinations of microhematocrit and white blood cell count. A 1-ml sample of whole blood was taken for Fe^{59} assay, and the remaining blood was centrifuged to obtain a 2-ml plasma sample. The γ-ray activity of the Fe^{59} in whole blood and in plasma was measured with a well-type sodium iodide crystal counter. An aliquot of the $Fe^{59}Cl_3$ injection solution served as the counting standard. The total Fe^{59} incorporated into the red blood cells was calculated by the method of Hennessey and Huff.[3]

After bleeding, the animals at the five higher dosage levels were autopsied, and the following tissues were dissected, weighed, and fixed in Zenker formol: mesenteric and cervical lymph nodes, thymus, spleen, liver, lung, kidney, ovary, adrenal, femur, small intestine (empty of contents), and gastric antrum.

Measurements of Ra^{223} and its daughters were made either on the γ-ray activity with a well-type sodium iodide crystal counter, or on the β activity with a G-M counter. Appropriate corrections were made for self-absorption. A standard was prepared for each experimental group. At the time of injection an accurately measured volume of each Ra^{223} solution was diluted to 100 ml in 2 $\underline{N}$ HNO_3, and an aliquot was assayed each time samples were counted.

RESULTS

Absorption, Excretion, and Retention

The results of the tracer study with Ra^{223} are shown in Table I. Uncomplexed Ra^{223} was absorbed somewhat slowly from the intramuscular injection site; 58% was absorbed in the first day. Later experiments indicated that addition of sodium citrate to the injection solution accelerated absorption to more than 90% in the first day.

After the first day the gastrointestinal tract was the chief route of elimination of Ra^{223}. Nearly two-thirds of the excreted Ra^{223} was found in the feces. Figure 1 shows the cumulative excretion--urinary, fecal, and total--of 0.006 μC/g of uncomplexed Ra^{223} for the first 18 days after injection. The cumulative total excretion of the group with lowest-level toxicity, 0.004 μC/g Ra^{223} complexed with sodium citrate, is shown in the same figure for comparison.

The rates of urinary, fecal, and total excretion of uncomplexed Ra^{223} in percent of adminstered dose per day could be represented by single-power functions for the first 16 days postinjection, as shown in Fig. 2. The equations of the regression lines of log E on log T are

$$\text{urinary excretion rate,} \quad E_u = 2.8\ T^{-0.76}, \tag{1}$$

$$\text{fecal excretion rate,} \quad E_f = 12.5\ T^{-1.08}, \tag{2}$$

$$\text{total excretion rate,} \quad E_t = 13.5\ T^{-0.95}, \tag{3}$$

where E is the percent excreted per day, and T is the number of days after injection. From the third to the 20th day after injection, the total excretion rate, 0.004 μC/g, of citrate-complexed Ra^{223} could also be represented by a power function with a slope similar to that for the total excretion of uncomplexed Ra^{223}. It is unlikely that the differences in the slopes of Eqs. (1), (2), and (3) are significant, inasmuch as the Ra^{223} in both the gastrointestional tract and the urine is derived from a common source, the circulating blood.

The effect of the amount of Ra^{223} administered on the excretion rate is shown in Fig. 3. The equations for the excretion rates of the various doses of Ra^{223} are given in the figure. Silberstein's data[4] for a dosage of 0.015 μC/g of Ra^{226} in male rats are shown for comparison. At the higher dosages a single-power function describes the decline in excretion rate for the 60-day observation period. The equation for the decline of the excretion rate with time for the 0.07-μC/g and 0.10-μC/g groups combined,

$$E_t = 14\ T^{-1.49}, \tag{4}$$

agrees fairly well with that obtained by Norris and Evans for 0.25 μC/g of Ra^{226} administered intraperitioneally to adult mice.[5] At our lowest injection level, 0.004 μC/g, the rate of excretion of Ra^{223} was better described by a series of exponentials (Fig. 4). The equation of the excretion curve for this lowest-level group was

$$E_t = 60\ e^{-1.38t} + 3.5\ e^{-0.30t} + 0.54\ e^{-0.019t}. \tag{5}$$

Table I

The deposition of radium-223 in the rat at 1, 8, and 16 days following intramuscular injection. Each rat received 1.5 microcuries of radium-223. Values are corrected for 100% recovery and expressed in percent of administered dose. The standard error of the mean for the liver and the skeleton is shown at the bottom of the table.

Tissue	Time after injection					
	1 day		8 days		16 days	
	% per organ	% per gram	% per organ	% per gram	% per organ	% per gram
Spleen	0.05	0.08	0.01	0.02	0.01	0.02
RBC	0.10	0.01	<0.01	-	<0.01	-
Plasma	0.21	0.03	<0.01	-	<0.01	-
Liver[a]	0.27	0.04	0.08	<0.01	0.07	0.01
Kidney	0.44	0.25	0.08	0.07	0.05	0.02
G-I tract	1.72	0.17	0.22	0.02	0.08	<0.01
G-I contents	8.21	-	1.17	-	0.44	-
Muscle	1.97	0.02	0.39	<0.01	0.68	<0.01
Femur	-	2.75	-	2.67	-	2.18
Tibia	-	3.00	-	3.54	-	2.79
Cranium	-	-	-	-	-	2.18
Costochondral junction	-	0.48	-	0.44	-	-
Skeleton[b]	63.4	3.41	53.3	2.83	46.7	2.27
Balance	1.98	-	1.14	-	0.45	-
Skin	0.89	0.03	0.22	<0.01	0.13	<0.01
Urine	8.65	-	15.0	-	17.6	-
Feces	12.1	-	28.3	-	33.6	-
Injection site	42.2		14.4		8.90	
Actual recovery	103.2		99.1		95.0	
[a]Mean std. error	± 0.02	±0.006				
[b]Mean std. error	± 0.6	± 0.05	± 0.76	± 0.08	± 0.55	± 0.06

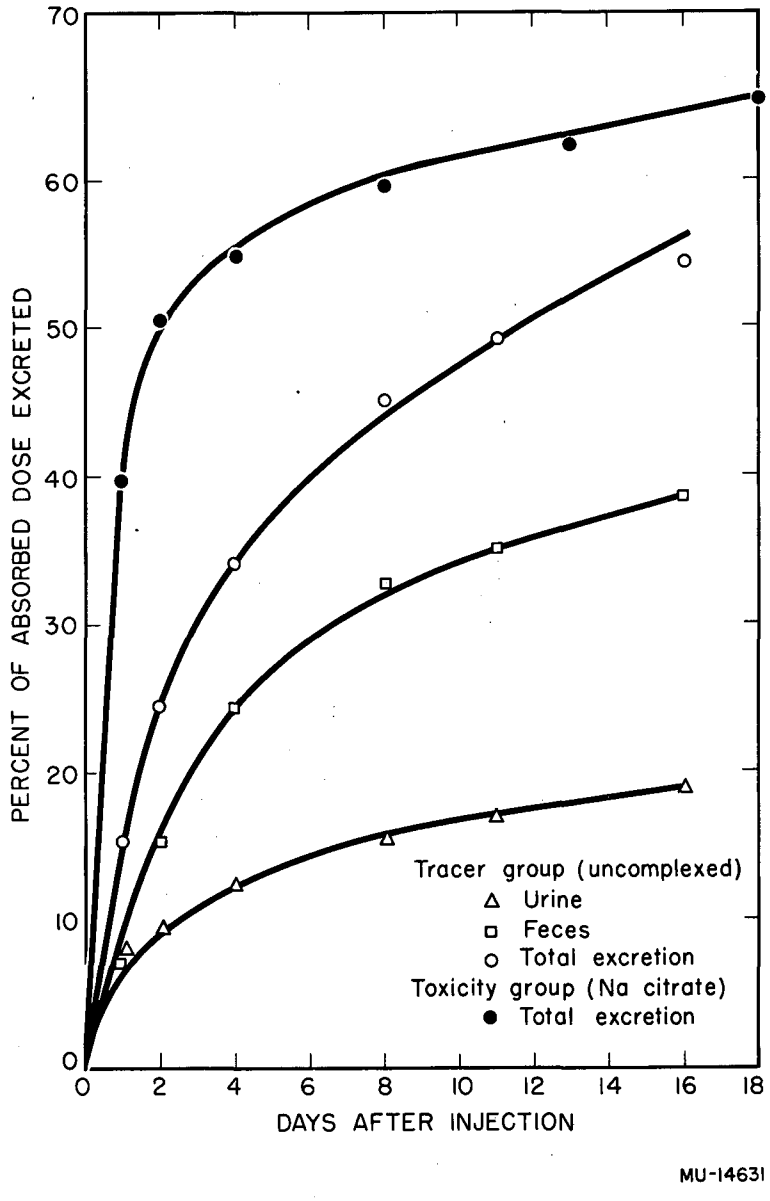

Fig. 1. Cumulative excretion of intramuscularly administered Ra^{223}.

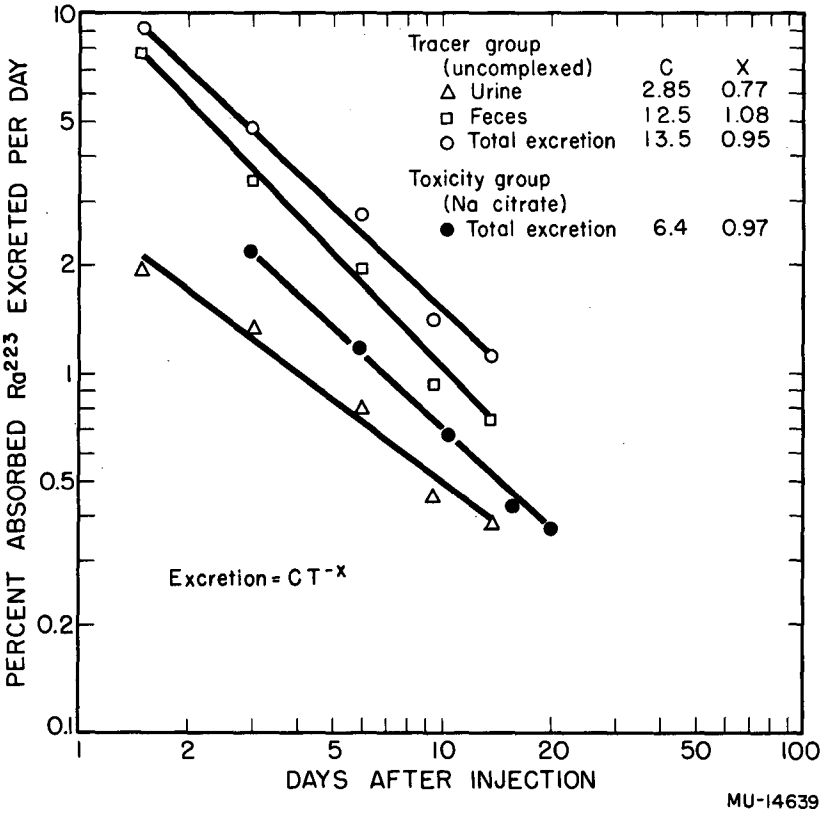

Fig. 2. Daily excretion rate of Ra^{223} represented as a power function.

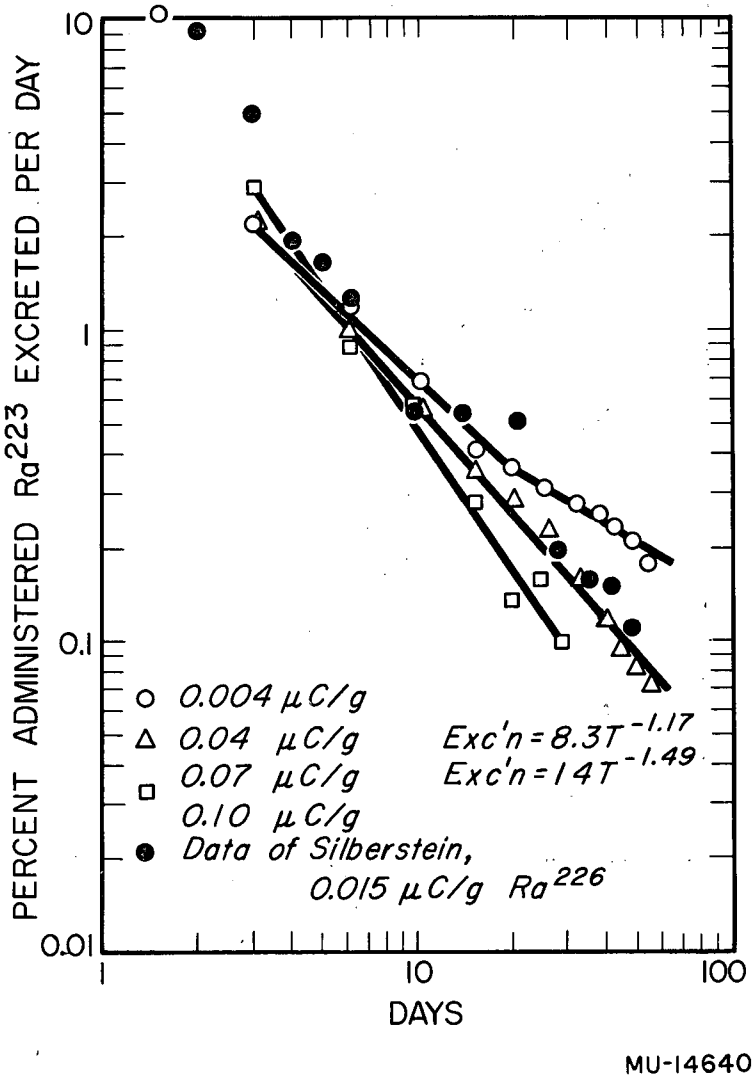

Fig. 3. Effect of the amount of Ra^{223} administered on the daily excretion rate. Data for Ra^{226} are from Silberstein.[4]

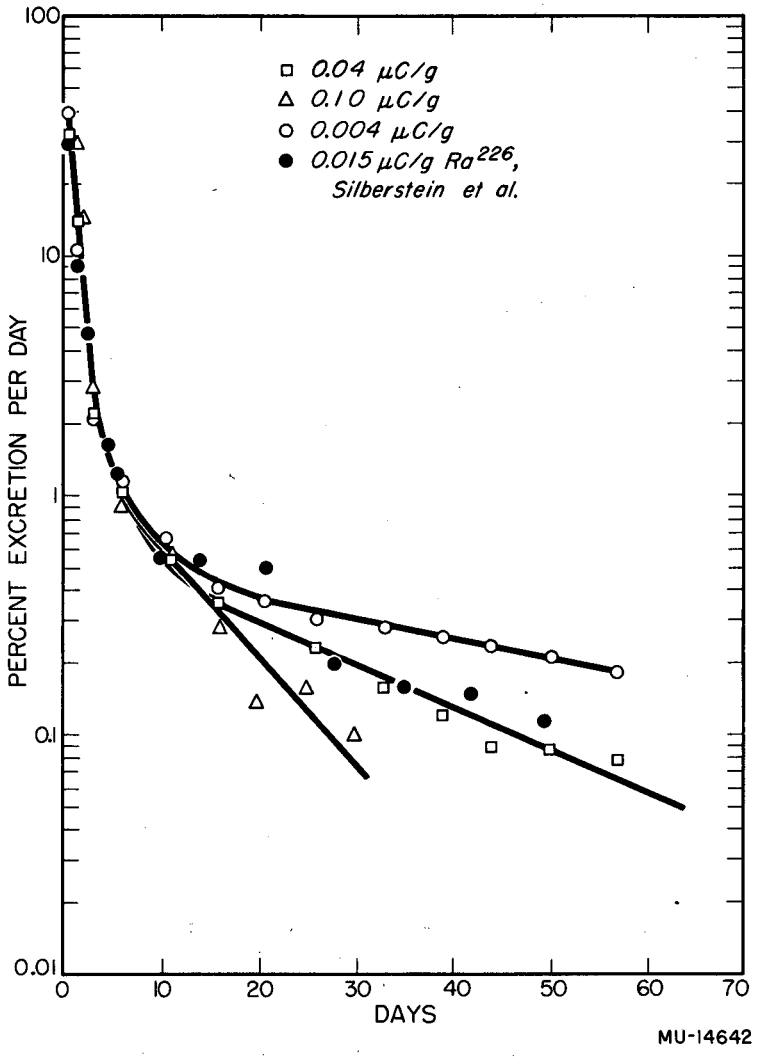

Fig. 4. The effect of the amount of Ra^{223} administered on the daily excretion rate, represented as a series of exponential functions. Data for Ra^{226} are from Silberstein.[4]

The accuracy of the excretion collection and sampling and the validity of the retentions calculated from excretion data are indicated by the recoveries of Ra^{223} from the excreta and carcasses of the high-level-toxicity rats that died from the 5th to the 30th day of the experiment. The recoveries for 23 animals (10 rats each from the 0.07-μC/g and 0.10-μC/g groups, two from the 0.04-μC/g group, and one from the 0.02-μC/g group) ranged from 91.8% to 103.1% of the administered dose, with a mean recovery of 98.4 ± 0.9%.

The dependence of Ra^{223} retention on the amount administered (presumably related to the radiation dose) can also be depicted by a power function as shown in Fig. 5 for 4 and 30 days postinjection. The equations of these lines are

$$R_4 = 62.3\ D^{0.063} \qquad (6)$$

and

$$R_{30} = 54.3\ D^{0.101}\ , \qquad (7)$$

where R is the percent of dose retained (obtained from excretion data) and D is the microcuries of Ra^{223} administered per gram body weight. Norris and Evans[5] found that Ra^{226} retention in male rats was related to dose by the equation

$$R = 57\ D^{0.177}\ . \qquad (8)$$

There are several complications involved in comparing our results with those of Norris and Evans:[5]

(a) There are differences in the skeletal growth patterns of male and female rats; after sexual maturity is achieved, the long bones of the male rat continue to grow at a more rapid rate than do those of the female.

(b) Norris and Evans measured the excretion of Ra^{226} at their highest injection level, 0.93 μC/g, and it would be expected from the results shown in Figs. 3 and 4 that the rate of excretion and total radium elimination, which are highly dose-dependent, would be the lowest for this high level of Ra^{226} administration.

(c) Because balance studies were not made, there are some uncertainties in Norris's and Evans's skeletal retention values.

In cases of accidental radium poisoning or contamination the quantity actually entering the body is usually not known. However, an estimate of the initial body burden can be made if the following information is available: (a) the rate of excretion at any time after contamination; (b) the time when contamination occurred; and (c) a curve obtained from animal experiments relating the fraction of the remaining body burden excreted per day to the time after administration. Figure 6 shows such curves for three dose levels of Ra^{223}. During the first 15 days after injection the curves for the three groups were quite similar. At the lowest level, 0.004 μC/g, the discontinuity first noted in the excretion curve (Fig. 2) is apparent. The equation relating the rate of change of the fraction of the body burden eliminated per day to the time after injection obtained by a least-squares fit was

$$F_{bb/d} = 0.168\ T^{-1.11} \qquad (9)$$

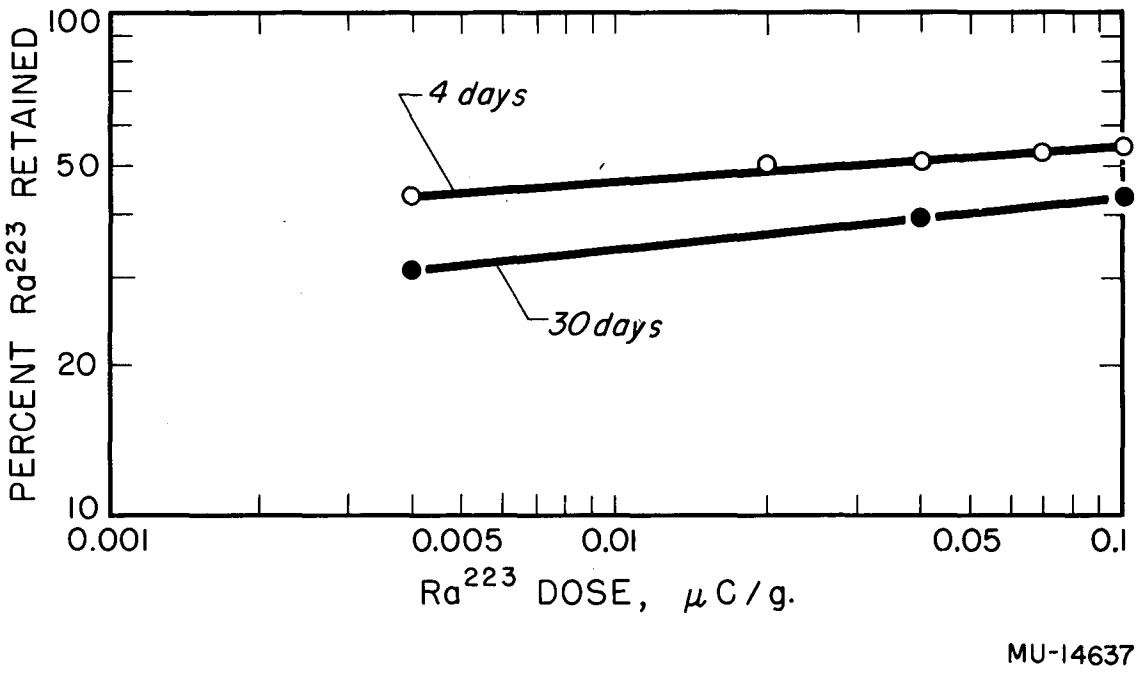

Fig. 5. The effect of the amount of Ra^{223} administered on retention (dose dependence of retention).

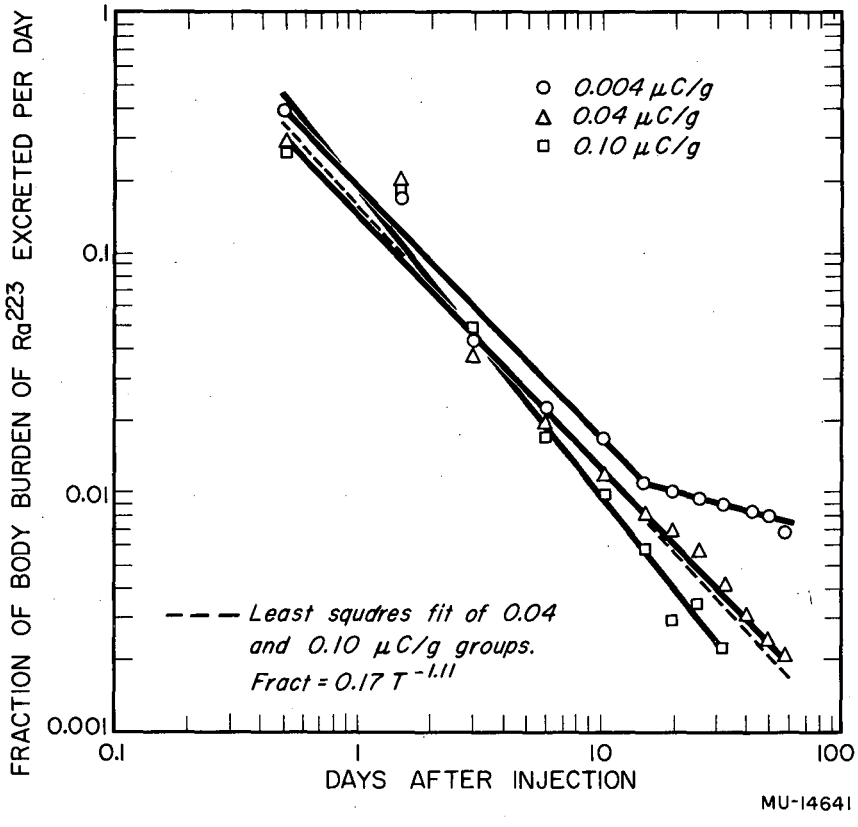

Fig. 6. The fraction of the Ra^{223} body burden excreted per day as a function of postinjection interval.

for all but the lowest injection level (the dashed line in the figure is the mean of the higher-level groups).

Distribution of Radium-223

The distribution of Ra^{223} in the soft tissues and several skeletal parts is shown in Table I. One day after injection, 8% of the retained Ra^{223} was distributed in the soft tissues exclusive of the contents of the gastrointestinal tract. By the 16th day the soft tissues contained only 3% of the retained Ra^{223}. Measurement of the Ra^{223} in the carcasses of the toxicity-study animals that died between the 16th and the 30th day showed that 1.6% of the retained Ra^{223} was still in the soft tissues. The bulk of the Ra^{223} was found in the skeleton. The concentrations in the skull cap and in the femur and tibia were similar, and by the 16th day were representative of the concentration in the entire skeleton.

Acute Toxicity of Radium-223 Mortality

The acute toxicity of Ra^{223} could not be represented in the customary fashion, relating mortality to the logarithm of the administered dose. At 30 days there had been no deaths at the lowest dosage level, 10% of the animals had died at the two medium levels, and all the high-dosage animals were dead. A plot of the 30-day percentage mortality vs dose (not shown) was a very steeply rising S-shaped curve with a mid-lethal point at about 0.05 $\mu C/g$ of Ra^{223}. The curve shape suggested a single mode of acute lethal action for this radioisotope.

The pattern of later deaths is shown in Fig. 7. At the lowest dosage level the death rate was not different from that of uninjected controls. Times longer than one year are not shown in the figure. Fourteen months after injection 60% of the 0.004-$\mu C/g$ rats were still alive.

As is shown later, some indication of the cause of the acute deaths can be obtained from the gross and microscopic pathology of the rats that were sacrificed 8 days after the Ra^{223} injections.

Acute Effects on Organ Weights

Table II shows the acute effects of Ra^{223} on the body weights and the autopsy weights of several tissues and organs. Those tissues that showed absolute losses in weight (compared with the tissues of the controls) were spleen, thymus, small intestine, and ovaries. Except for the ovaries, these tissues showed weight losses out of proportion to the loss of body weight, so that an actual depletion can be inferred. This was borne out by microscopic examination of the spleen and thymus.

The effect of increasing levels of Ra^{223} on body weight and on weights of spleen, thymus, and small intestine is shown in Figs. 8 through 11. Tissue weights are expressed as percentages of normal control weights. Spleen, thymus, and body weights appeared to be linear functions of dose under the experimental conditions described here. Storer et al. have shown that 3 to 5 days after whole-body x-irradiation, the spleen and thymus lost weight exponentially with increasing dose.[6] Our data for percent reduction in spleen, thymus, and body weights, replotted as functions of log dose, are shown in Fig. 12. The linearity of the relationship between percent weight loss and

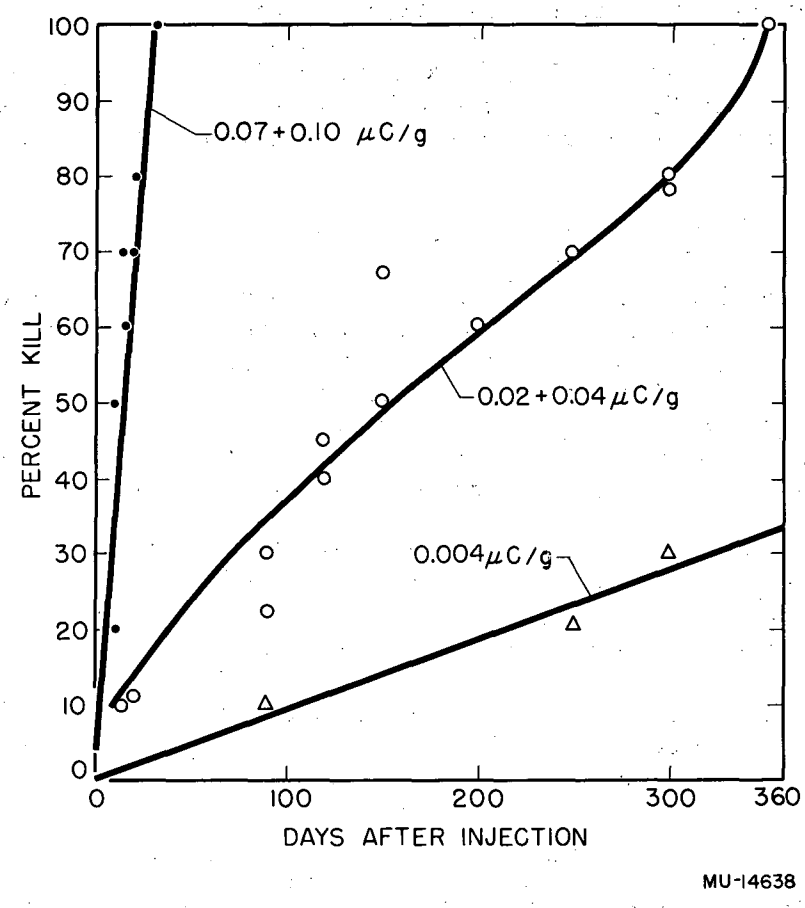

Fig. 7. The effect of varying levels of Ra^{223} administration on the life span of the rat.

Table II

The effect of various dosages of Ra^{223} on the body weight and weights of several organs of the rat 8 days after administration. Mean weights are shown with the standard error.[a]

Group	No. rats	Body weight (g)	Organ Weight (g)							
			Spleen	Thymus	Small bowel	Adrenals	Ovaries	Kidneys	Femurs	Liver
Control	10	240±3	0.52±.03	0.31±.02	3.9±.16	0.062±.002	0.092±.009	1.8±.05	2.1±.05	7.0±.27
0.004 μC/g	11	243±8	0.47±.02	0.32±.05	3.1±.16	0.065±.002	0.081±.007	1.8±.06	2.1±.06	6.8±.28
0.02 μC/g	11	240±8	0.47±.03	0.31±.05	3.4±.25	0.064±.004	0.072±.003	1.8±.08	2.2±.07	7.0±.26
0.04 μC/g	11	220±6	0.42±.04	0.23±.02	2.6±.21	0.072±.003	0.076±.003	1.8±.05	2.2±.05	7.5±.19
0.07 μC/g	10	208±10	0.31±.02	0.13±.02	2.3±.31	0.074±.004	0.067±.004	1.8±.05	2.1±.05	8.0±.21
0.10 μC/g	11	205±4	0.26±.01	0.16±.01	2.6±.21	0.076±.005	0.067±.006	1.7±.08	2.1±.04	8.4±.26

[a] $S.E. = \sqrt{\frac{\sum (dev.)^2}{n(n-1)}}$

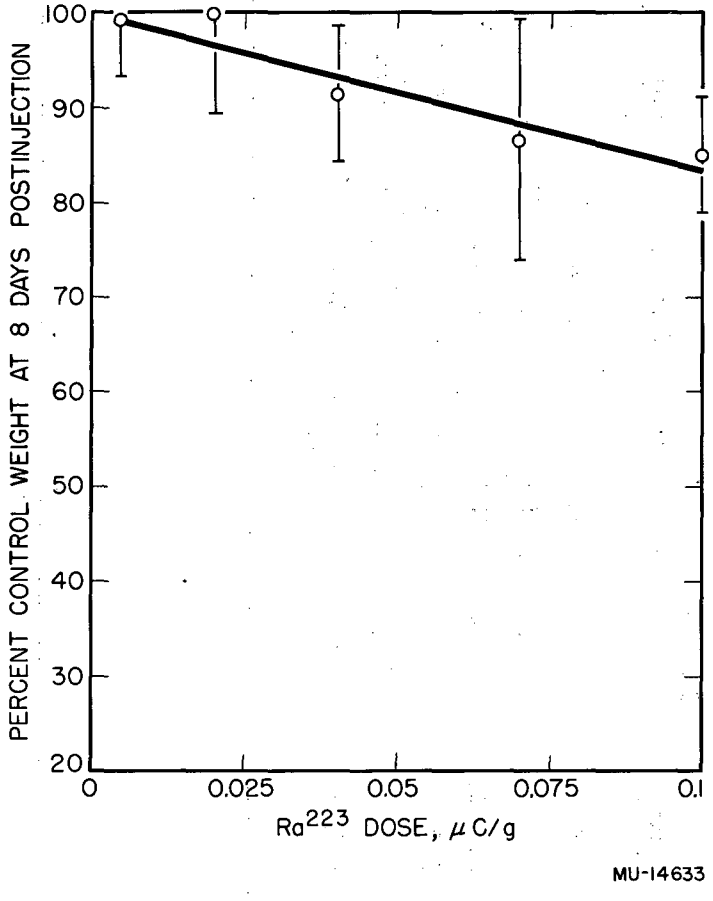

Fig. 8. The effect of Ra^{223} on the body weight of the rat. Measurements taken on the 8th postinjection day.

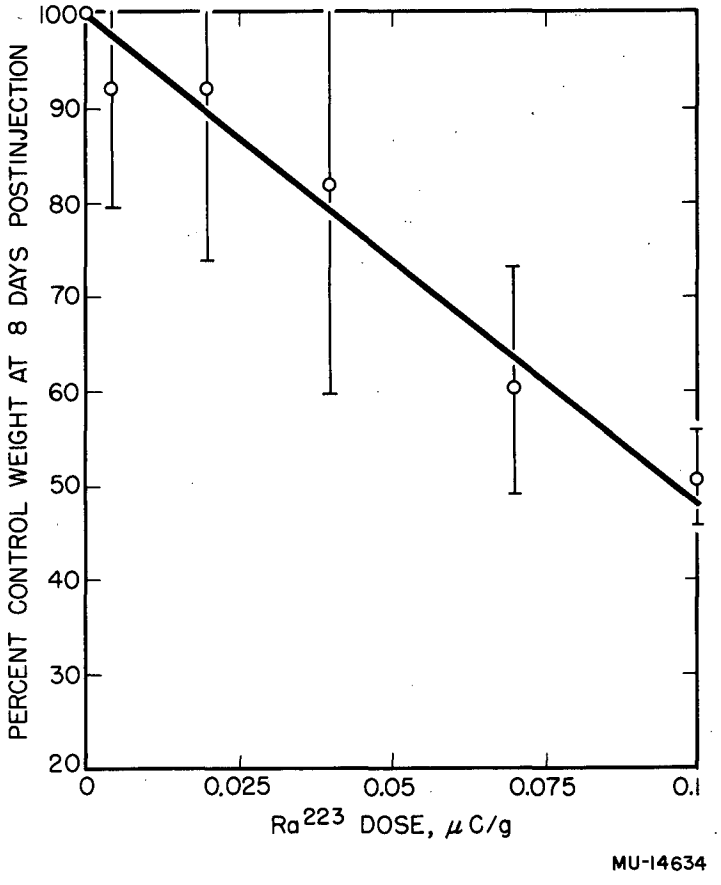

Fig. 9. The effect of Ra^{223} on spleen weight. Measurements taken on the 8th postinjection day.

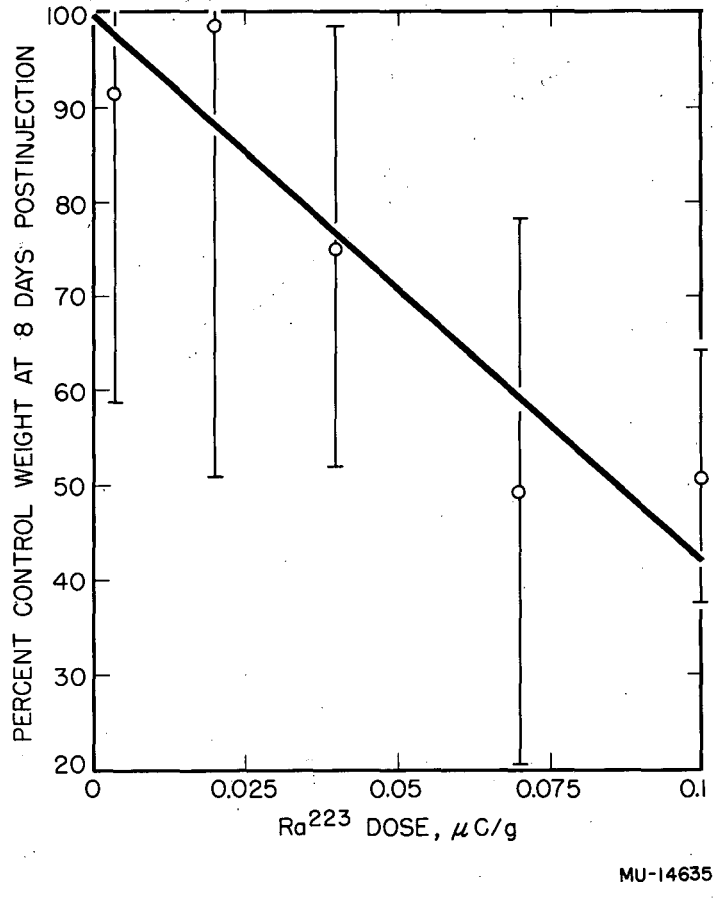

Fig. 10. The effect of Ra^{223} on thymus weight. Measurements taken on the 8th postinjection day.

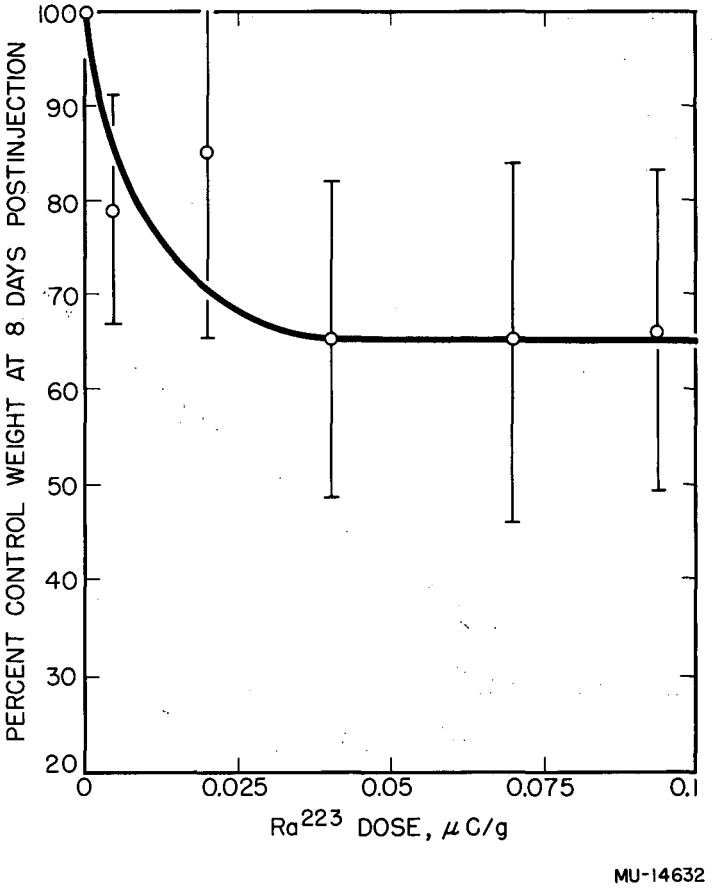

Fig. 11. The effect of Ra^{223} on weight of the small intestine. Measurements taken on the 8th postinjection day.

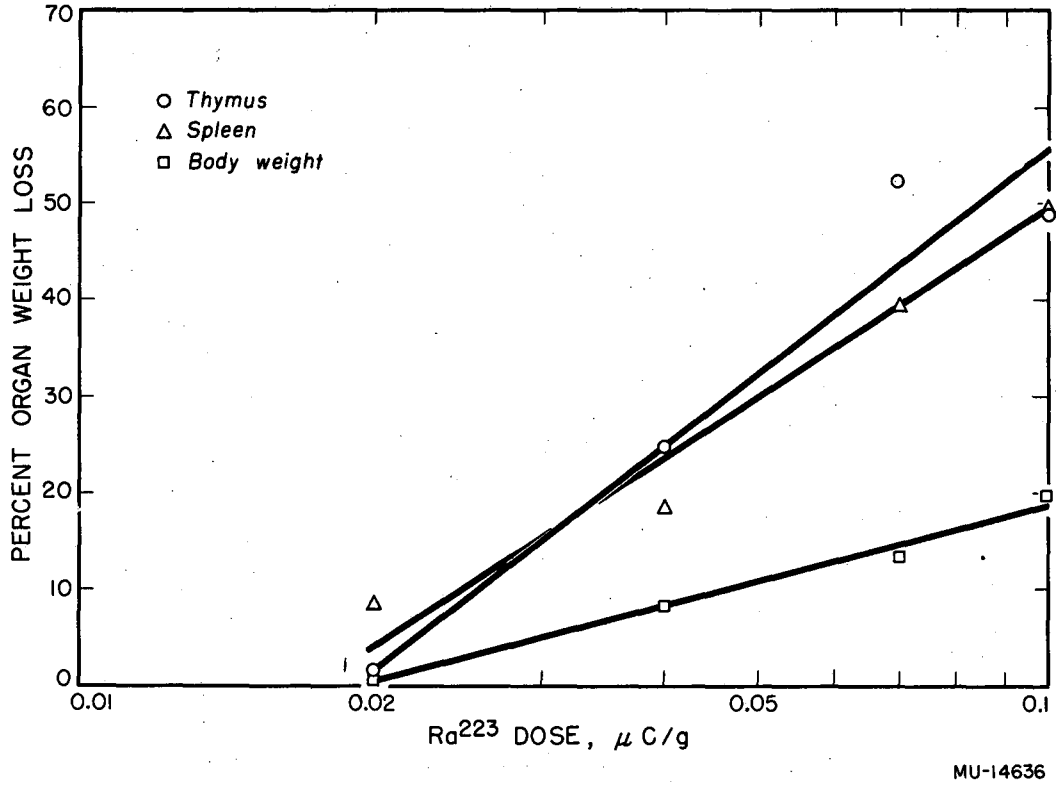

Fig. 12. The percentage loss in body weight and spleen and thymus weights shown as exponential functions of the Ra^{223} dose.

dose is not certain, because (a) the least-squares fits and the best eye fits did not agree well, and (b) as shown in the previous figures, the individual measurements varied widely.

The weight of the small intestine was nearly a constant percentage of the control value, 65%, at Ra^{223} levels greater than 0.04 μC/g. The gross autopsy findings suggested that the decrease in intestinal weight at 8 days postinjection was chiefly due to substantial reduction in both the size and number of Peyer's patches rather than to the atrophy or denudation of the intestinal mucosa that has been observed after whole-body x-ray.[7]

The weights of the kidneys, femurs, and adrenal glands were the same as those of the controls, so that when body weight had been lost at the higher Ra^{223} levels they constituted a larger percentage of the body weight. Above the 0.04-μC/g level the livers of the Ra^{223}-treated rats were actually heavier than those of the controls. The weight increase was probably due to interlobular edema and swelling of the hepatic cells, both of which were seen microscopically.

Acute Gross Pathology

Grossly, the animals showed a progressively more severe hemorrhagic condition with increasing Ra^{223} dose. At the lowest dose level, five of the eleven animals revealed small discrete hemorrhagic areas in the cervical and mesenteric lymph nodes, six showed a few punctate hemorrhages in the thymus, and in four specimens a few very small petechial hemorrhages were seen in the gastric antrum.

At the next dosage level, 0.02 μC/g, the findings were nearly the same as for the previous group except that 9 of the 11 specimens showed the hemorrhages in the periphery of the lymph nodes, and the Peyer's patches seemed somewhat reduced--both in size and in number.

At the next Ra^{223} level, 0.04 μC/g, 10 of 11 specimens showed some hemorrhage in the lymph nodes, and in six rats the cervical and mesenteric nodes were nearly uniformly hemorrhagic. In eight rats the thymi were irregularly hemorrhagic, and the mediastinal lymph nodes were uniformly so. The size and number of the Peyer's patches were substantially reduced. Numerous petechial hemmorhages were found in the gastric mucosa of these animals, and one animal was bleeding into the gastric lumen. The lungs of three animals were hemorrhaging, as evidenced by blood on their muzzles and paws.

At the two highest levels, 0.07 μC/g and 0.10 μC/g, the lymph nodes and thymi of all 21 animals were moderately to heavily hemorrhagic. Very few, if any, Peyer's patches were seen in any of the animals, and those present were only tissue remnants. Numerous petechial hemorrhages were found in the gastric mucosae of all animals at these dose levels. Two-thirds of the animals showed blood in the stomach, either from massive bleeding into the gastric lumen or from swallowing of blood from the lungs. The hematocrits of the animals that were bleeding heavily were less than 0.20.

Microscopic Pathology of Group B

Spleen

Somewhat reduced lymphopoietic activity was consistently noted in the spleen above the 0.02-μC/g level. At the 0.04-μC/g and 0.07-μC/g levels the reduction was moderate, and at the highest level depletion was extensive. Necrotic debris was frequently found in the germinal centers. Even at the highest dose level many germinal centers could be found that appeared to be functional, but the over-all picture was an abnormal one--more severe with increasing Ra^{223} dose. The white pulp of the spleen appeared somewhat more resistant than the germinal centers, although a definite decrease in lymphocyte content was observed at the three higher dose levels. At these latter dosages there seemed to be a tendency toward excessive packing of erythrocytes in the splenic red pulp. The splenic macrophages generally contained more golden-brown pigment than was seen in the control specimens.

Thymus

Above the 0.04-μC/g level the thymic cortex was markedly reduced in size, and lymphocytes were sparse. In some specimens the cortex contained necrotic cellular debris, while in others the debris was found mainly in the medullary stroma. At the higher dose levels a moderate hemorrhagic infiltration was seen in the cortical lymphatic tissue. In a few cases erythrocytes were undergoing phagocytosis.

Lymph Nodes

At the lower Ra^{223} dosage levels the mesenteric lymph nodes showed changes more frequently than did the cervical or axillary nodes. In the mesenteric nodes the cortical lymphatic tissue was somewhat reduced even at the lowest dosage, 0.004 μC/g. Hemorrhagic infiltration and decreased lymphocyte content became more frequent and more severe with increasing dose. Similar changes were observed in the cervical nodes at the three high dose levels, along with a reduction in the size of the cortical lymphatic follicles. At the two highest dosages necrotic cellular debris was seen in the centers of some follicles. Some of these specimens showed an early fibroblastic proliferation in the cortex as well as in the hilar areas, but this phenomenon was usually limited to a single area. Hemorrhagic infiltration, occasionally with active phagocytosis, was most frequent and most extensive at the 0.07-μC/g and 0.10-μC/g levels. Fresh infiltrations were seen most often in the peripheral lymph sinuses, whereas the older hemorrhages were generally located in the medullary stroma.

Bone Marrow

Decreased cellularity of the bone marrow was seen at the two lowest dose levels, but the most marked and consistent changes were found at the higher levels, at which marrow cells were almost completely absent. The marrow in the epiphysis and just below the epiphyseal plate was always more severely damaged than that deep in the center of the shaft. The megakaryocytes seemed to disappear from the marrow at lower dosage levels than did the other marrow cells.

Stomach

Changes in the gastric mucosa were minimal below the 0.04-μC/g level. Above this dosage the mucosa contained small areas of necrotic cells in the superficial glands, with some ulceration of the mucosal surface. At the two highest levels the deeper glandular tissue was often seen in the early stages of degeneration; the nuclei were pyknotic, the cell membranes were disrupted, and the cytoplasm was degenerating with sloughing of the degenerated superficial tissues. The plane of sectioning may explain why hemorrhage into the mucosa was seen in only one specimen, whereas frank bleeding was a common gross observation.

Liver

In several liver specimens at the 0.04-μC/g level, and in most specimens at higher Ra^{223} dosages, small vacuoles (often multiple) were found in the cytoplasm of the parenchymal cells but without accompanying nuclear changes. These vacuolated cells were usually restricted to the peripheral portions of the lobules, but occasionally the cells of an entire lobule were involved. The presence of a pale-staining reticulum within the vacuoles suggests hydropic degeneration resulting from the anoxia associated with the severe hemorrhage, poor nutrition, an acute infection, or a combination of the foregoing.[8] Imbibition of excess water by the parenchymal cells of the liver would also account for the observed absolute increase in liver weight. At the three highest dose levels cell degeneration was common. The nuclei were pyknotic, the cell walls were disintegrating, and the cytoplasm was clumped and disintegrating. These changes were most prominent in the peripheral areas of lobules and were not always related to the vacuolization.

Adrenals

The changes in the adrenal glands are questionable because of their poor preservation or damage in processing. Early degenerative changes in the fasciculata seemed to be relatively prominent at the higher dosages, following which pyknotic nuclei and cytoplasmic degeneration were observed with some frequency. At the highest dose level small vacuoles (often multiple) were seen in the cytoplasm of some cells in the zona fasciculata.

Kidney

The renal glomeruli were occasionally atrophic and avascular at the higher dosages, with pyknotic nuclei and condensed supporting tissues. Degeneration, with loss of cytoplasm and with partial to total obliteration of the tubular lumens, was often seen in the proximal convoluted tubules at all but the lowest dose level. There did not seem to be a correlation between the extent of renal damage and increasing dose of Ra^{223}. For the most part the distal and collecting tubules were intact, but occasionally they were distended with a basophilic exudate, and there were small localized areas of tubular degeneration.

Acute Effects of Radium-223 on Bone Marrow

There was significant depression of the amount of an Fe^{59} tracer incorporated into the red cells at all Ra^{223} dosage levels above 0.002 μC/g. The mean percentages of Fe^{59} uptake at various Ra^{223} dosages are shown in Table III. Measurements taken on animals that were obviously hemorrhagic, or whose hematocrits were less than 60% of normal, were not included in the group shown in the table or in the figures that follow.

A semilogarithmic plot of percent normal Fe^{59} uptake vs Ra^{223} dose (in μC/g) yielded a two-component curve (Fig. 13) with the equation

$$\% \text{ normal } Fe^{59} \text{ uptake} = 32\% \, e^{-385 \, d} + 68\% \, e^{-20 \, d}. \quad (9)$$

The histological appearance of the 8-day femurs should be mentioned at this point, although more detailed descriptions appear elsewhere. At low Ra^{223} dosages cellular marrow had disappeared from the epiphyses and from the neighborhood of bony trabeculae; however, a cylindrical core of apparently normal marrow was still present deep in the center of the shaft except at the very highest dosages. It is tentatively suggested that the initial steep component of the curve shown in Fig. 13, which represents destruction of about 30% of the total marrow, is a measure of the direct irradiation of marrow immediately adjacent to the bony surfaces where Ra^{223} had been deposited. The process responsible for the second component, which is less sensitive to the Ra^{223} dosage, has not been established, but is discussed in a later section.

Figure 14 shows the percent of normal Fe^{59} uptake in the red cells plotted as a function of the radiation dose (in rad) according to the method of Storer et al.[6] A straight line could be drawn over the range of dosages from 45 to 4500 rad. The equation of this line (fitted by the method of least squares) was

$$Y = 42.2 \log X + 166, \quad (10)$$

where Y is the percent normal Fe^{59} uptake, and X is the radiation dose (in rad) accumulated in the first 5 days after the Ra^{223} injection. The same figure shows data from Storer et al. for a body burden of tritium sustained for 2 days.[6] The equation for their data was

$$Y = -79.6 \log X + 209. \quad (11)$$

Hennessey and O'Kunewick have shown that the Fe^{59} in the circulating red cells is a measure of the functional state of the marrow at the time Fe^{59} is injected;[9] therefore, the radiation dosages shown in Fig. 14 represent the radiation accumulated on the day of the Fe^{59} injection, the second day with H^3, and fifth day for Ra^{223}. The slopes of the curves for H^3 and Ra^{223} are so different that an estimate of relative biological effectiveness (RBE) could not be made for this particular test system without taking into account the irregular radiation pattern of radium.

The data shown in Fig. 13 for Fe^{59} uptake vs Ra^{223} dosage (in μC/g) were replotted in Fig. 15 as a function of the accumulated radiation.

Table III

The effect of Ra^{223} on the incorporation of Fe^{59} into the red blood cells

Dose Ra^{223} ($\mu C/g$)	No. rats	5-Day integral marrow dose(rad[a])	% dose Fe^{59} ± S.E.	% normal Fe^{59} ± S.E.
0	22		49.9 ± 2.3	100
0.004	10	16.8	49.1 ± 1.4	98.4 ± 5.3
0.001	10	42	48.5 ± 1.1	97.2 ± 5.0
0.002	7	82	45.2 ± 2.3	90.6 ± 6.2
0.003	10	126	37.2 ± 1.3	74.5 ± 4.3
0.004	15	168	35.0 ± 2.4	70.1 ± 5.8
0.008	10	336	27.2 ± 0.8	54.5 ± 3.0
0.02	11	840	25.7 ± 3.9	51.5 ± 8.2
0.04	11	1850	16.8 ± 4.2	33.7 ± 5.4
0.07	7	3300	7.72 ± 2.4	15.5 ± 4.7
0.10	9	4700	3.82 ± 0.7	7.66 ± 1.4

[a]The radiation dosages given were calculated according to the method described in the Appendix.

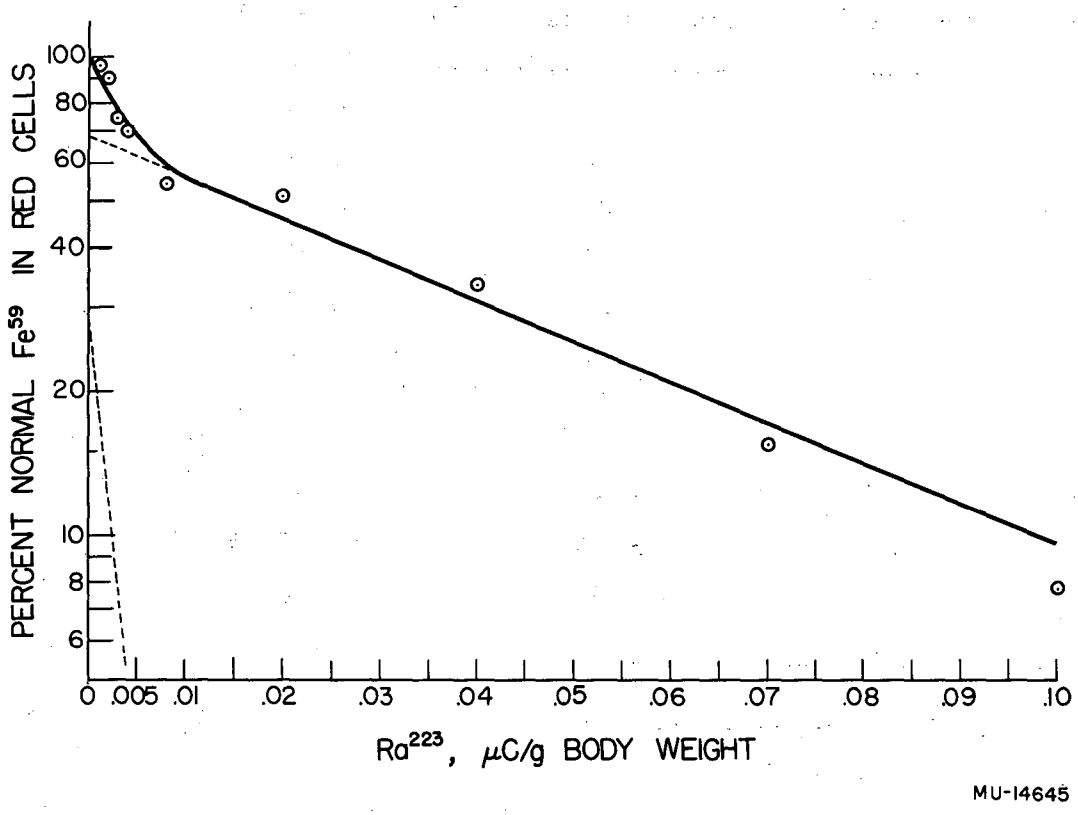

Fig. 13. The effect of varying levels of Ra^{223} on the incorporation of a tracer dose of Fe^{59} into the circulating red blood cells.

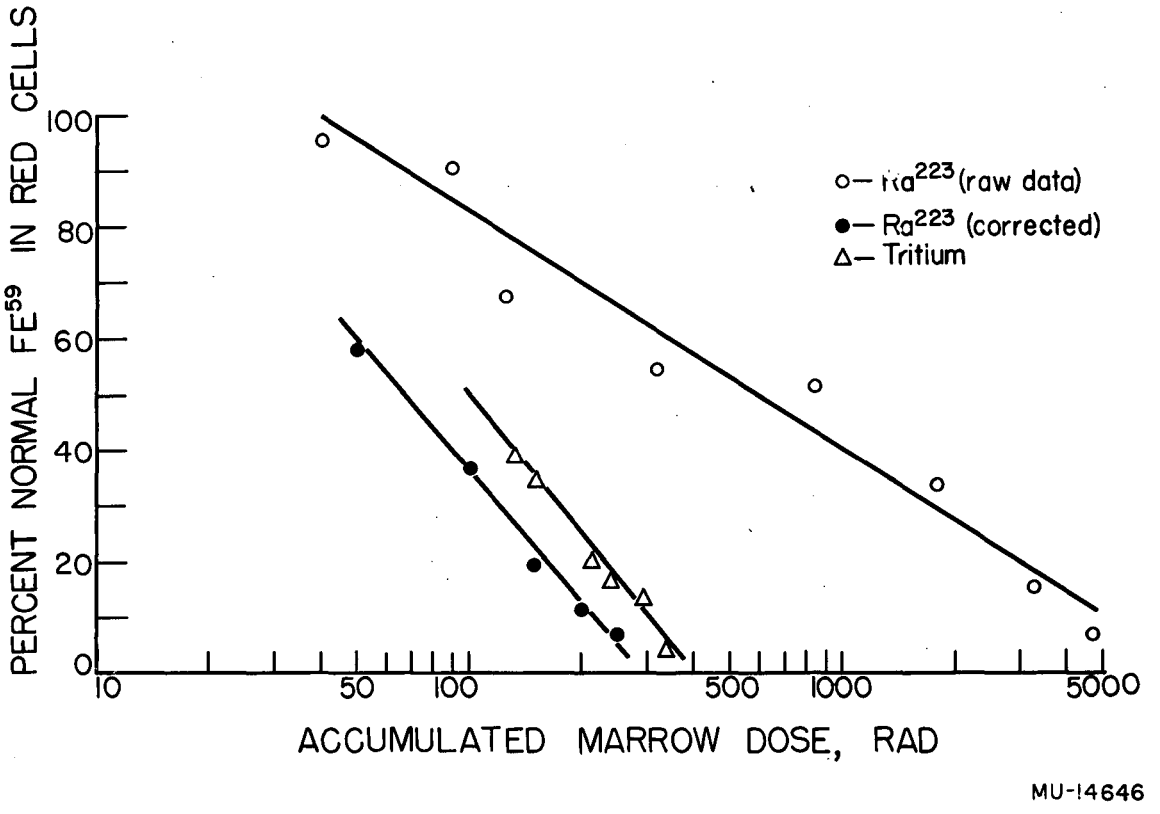

Fig. 14. The depression of Fe^{59} uptake in the red blood cells by varying levels of Ra^{223}, shown as a function of the calculated radiation dosage in the bone marrow (see Appendix for method of dosage calculation). Data for tritium are from Storer et al.[6]

Geometrical analysis of Fig. 15 yielded an initial component with an intercept at 29% Fe^{59} uptake. The 29% was assumed to represent that fraction of the red cell precursors destroyed by direct action of the Ra^{223} alpha particles. Fractional values were then read from Fig. 15 for dosages ranging from 50 to 250 rad. For example, at 200 rad, the percent normal Fe^{59} uptake was 3.3/29 = 11.4%. The regression line for reduction of Fe^{59} uptake in the directly irradiated marrow is shown in Fig. 14, and has the equation

$$Y = -79.4 \log X + 19. \quad (12)$$

The slope of the adjusted Ra^{223} curve was the same as that for Storer's tritium data.[6] The similarity of the slopes allowed us to estimate an RBE for Ra^{223} alpha particles compared to tritium beta particles as 1.509, and for Ra^{223} compared to Co^{60} γ rays, RBE = 1.509 x 1.593 = 2.40 (see Storer et al. for the method of calculation of RBE from data of this type). It should be emphasized that this calculated value of the RBE of Ra^{223} α: Co^{60} γ is not a precise quantity. If one takes the rate of dose delivery into account (the tritium β and Co^{60} γ radiation were delivered in 2 days and the Ra^{223} α in 5 days) the RBE may be somewhat greater. If the Ra^{223} irradiation dose had been calculated for only the marrow volume within one alpha-particle range of the bony surfaces instead of the entire marrow mass, the estimated RBE would be smaller. These compensating errors no doubt contributed to the close agreement between our data and that of Storer et al.[6]

The Effect of Ra^{223} on the White Blood Cells

There was a marked depression of the total white cell count involving both the lymphocytes and granulocytes following administration of even small amounts of Ra^{223}. Table IV shows the total white cell count and the percentage of granulocytes for a range of Ra^{223} dosages. These counts were taken 6 to 8 days after the Ra^{223} injection, the postinjection time at which both lymphocyte and granulocyte counts were minimal. The white cell count proved to be the most sensitive indicator of radiation effect. At the very low dosage of 0.001 μC/g of Ra^{223}, the animals appeared normal in all respects; however, the white cell count was significantly lower than the mean for the controls ($P < 0.01$).

Reduction of the granulocyte count plotted semilogarithmically as a function of the calculated bone marrow dose (in rad) is shown in Fig. 15. The equation of this curve is

$$\%\ \text{normal granulocyte count} = 78\%\ e^{-0.0126\ \text{rad}} + 20\%\ e^{-0.00138\ \text{rad}} + 1.6\%. \quad (13)$$

Yoffey indicates that in the guinea pig (and presumably other rodents) the marrow contains 100 times as many granulocytes as are present in the circulating blood, and is the storage depot for more than 95% of the mature granulocytes.[10] The initial component of the above equation is therefore presumed to represent direct irradiation damage of both the granulocyte precursors and the stored mature cells. The source of the less dosage-

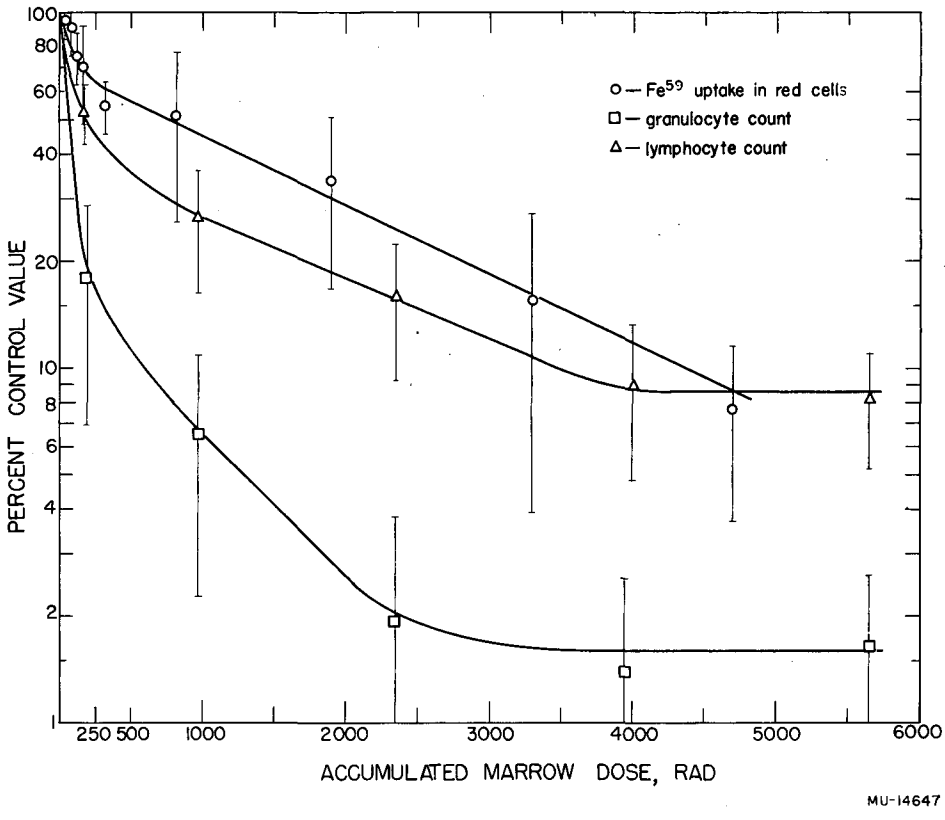

Fig. 15. The effect of varying levels of Ra^{223} administration on the uptake of Fe^{59} in the circulating red cells and on the lymphocyte and granulocyte counts of the peripheral blood, shown as functions of the calculated radiation dosage in the bone marrow (see Appendix for method of calculation).

Table IV

Effect of Ra^{223} on total white cell and differential white cell count

Ra^{223} dose ($\mu C/g$)	No. rats	Days post-injection	Accumulated radiation dose in marrow (rad)	Total WBC ± S.E.	% granulocytes
Control	12	8	0	8860 ± 780	
0.004	10	8	23.6	6730 ± 750	
0.001	10	8	56.5	5320 ± 130	
0.002	10	8	113	4470 ± 500	
0.003	10	8	170	3350 ± 260	
0.004	10	8	236	3400 ± 240	
0.008	10	8	452	2160 ± 140	
Control	45	6-7	0	13,260 ± 590	11.5 ± 0.8
0.004	10	6-7	198	6130 ± 580	3.5 ± 0.9
0.02	10	6-7	985	2580 ± 300	3.9 ± 0.7
0.04	10	6-7	2360	1960 ± 200	1.5 ± 0.3
0.07	10	6-7	3940	1110 ± 140	2.1 ± 0.4
0.10	8	6-7	5650	760 ± 80	1.9 ± 0.6

sensitive second component is not clear.* The flat portion of the curve is believed to represent those cells in the circulation before the Ra^{223} was injected.

Figure 15 also shows the effect of Ra^{223} on the circulating lymphocytes. Lymphopenia has been observed by others following the administration of Sr^{89},[11] or natural radium.[12] The phenomenon is difficult to explain, as soft-tissue dosages from radioisotopes of the alkaline earth elements are quite small. After intravenous injection of Sr^{90}- Y^{90} or old Ra^{226} the lymph nodes and spleen receive rather heavy irradiation from the Y^{90} daughter of Sr^{90} and from polonium present in the old radium preparations, but very little radiation from the strontium or radium isotopes themselves.[12] For Ra^{223} the problem is even more puzzling, since the radioactive daughters have half lives of less than 36 min, and radiation from the daughters (with independent metabolic pathways) present in an injected equilibrium mixture is insufficient to account for more than a few rad delivered to soft tissue.

The lymphocyte count is sensitive to many bodily disturbances. It is depressed in hypothyroidism,[13] hyperadrenalism,[14] and severe malnutrition,[15] is increased in chronic infections, and temporarily increased following splenic contraction under nervous stimulation.[16] However, factors of this nature cannot account completely for the marked and prolonged lymphopenia observed in animals internally irradiated with radioisotopes of the alkaline earths. It should be mentioned (see section on acute pathology) that except for the two highest Ra^{223} dosage levels, and apart from the severe hemorrhage in all the lymphatic tissues, lymphocyte depletion was the most consistent microscopic finding in the spleen, lymph nodes, and thymus. Yoffey's observations on the marrow of the guinea pig are of interest at this point.[10] His work shows that in this species the bone marrow is one of the major storage depots for mature lymphocytes. Preliminary experiments in our laboratory indicate that lymphocytes comprise about 40% of the total free cells of the marrow in the 200-day-old female rat as determined from differential cell counts in marrow smears. Lymphocytes are 23 times as numerous in the bone marrow of the guinea pig as in the circulating blood, and they equal eight times the normal daily thoracic-duct output. Yoffey also observed a centripetal movement of lymphocytes from the lymph nodes into the marrow. Trowell has emphasized the marked radiosensitivity of the small (mature) lymphocyte.[17] One may then attempt to explain at least in part the pronounced decline of circulating lymphocytes in a situation where more than 95% of the internal radiation is being delivered to the bone and bone marrow.

Graphic analysis of the curve for lymphocyte count vs marrow dose (Fig. 15) yielded the equation

$$\%\ \text{normal count} = 33\%\, e^{-0.015\ \text{rad}} + 21\%\, e^{-0.0051\ \text{rad}} + 37.5\%\, e^{-0.00071\ \text{rad}} + 8.6\%.$$ [14]

*A more detailed determination of this curve should allow resolution into at least four components if the stem cells and mature forms differ markedly in radiosensitivity.

Although it is not possible with the information at hand to match individual components with specific biological processes, the similarity of the slopes of the initial components of all three curves shown in Fig. 15 (Fe^{59} uptake, $-0.0106\ rad^{-1}$; granulocyte count, $-0.012\ rad^{-1}$; lymphocyte count, $-0.015\ rad^{-1}$) suggests a common process, namely, direct radiation damage of erythrocytic and granulocytic precursor cells and of mature granulocytes and lymphocytes.

Continued destruction of the mature lymphocytes that have migrated to the marrow, probably accompanied at higher Ra^{223} dosages by a decline in lymphocyte production resulting from poor general nutrition and some tissue destruction, could account for the observed depletion of the lymphatic tissues and for the decline in the number of circulating cells. The presence of necrotic cellular debris, particularly in the mesenteric nodes (the cervical nodes were invariably more normal in appearance) at the very highest Ra^{223} levels, suggests at least a small contribution from direct radiation damage. (It is not unlikely that some of the Ra^{223} that passes into the intestinal lumen, and is reabsorbed, making its way back into the circulation via the intestinal lymphatics and the mesenteric nodes thus exposes them at high levels of Ra^{223} administration to a significant radiation dose.)

Chronic Effects of Radium-223

The effect of a single injection of Ra^{223} on body weight is shown in Fig. 16. In general the animals that died after the 60th postinjection day suffered a precipitous weight loss in the 30 days immediately preceding death. The mean weights shown in the figure represent only those animals alive 30 days prior to the date of weighing.

Even at the lowest injection level, 0.004 μC/g, there was a slight weight loss immediately after the Ra^{223} administration. During the succeeding 2 months growth apparently resumed, and these animals maintained normal body weights until very nearly the end of their life span. At the medium doses, 0.02 μC/g and 0.04 μC/g, there was a somewhat greater initial weight loss followed by a temporary recovery. From the second to the fourth month, the interval in which most of the deaths occurred in these two groups, there was another period of weight loss even more severe than that immediately after the injection. Those animals that survived past the fourth month regained most of the weight lost in the preceding months, but failed to grow beyond preinjection weight. Another period of weight loss preceded the deaths of the remaining animals between the 9th and 11th months postinjection. At the highest injection levels the body weights declined sharply until death.

Chronic Effects on Erythropoiesis

The long-term sequelae of a single injection of Ra^{223} on the red cell count, hemoglobin level, and hematocrit (H, R, H) of the rat are shown in Figs. 17a, 18a, and 18b respectively. At all dosages there was a marked rise in these H, R, H's during the first week after injection, probably reflecting hemoconcentration. At the lowest dosage level the H, R, H had fallen to the lower limits of normal by the 30th day. Until the 400th day the erythrocyte

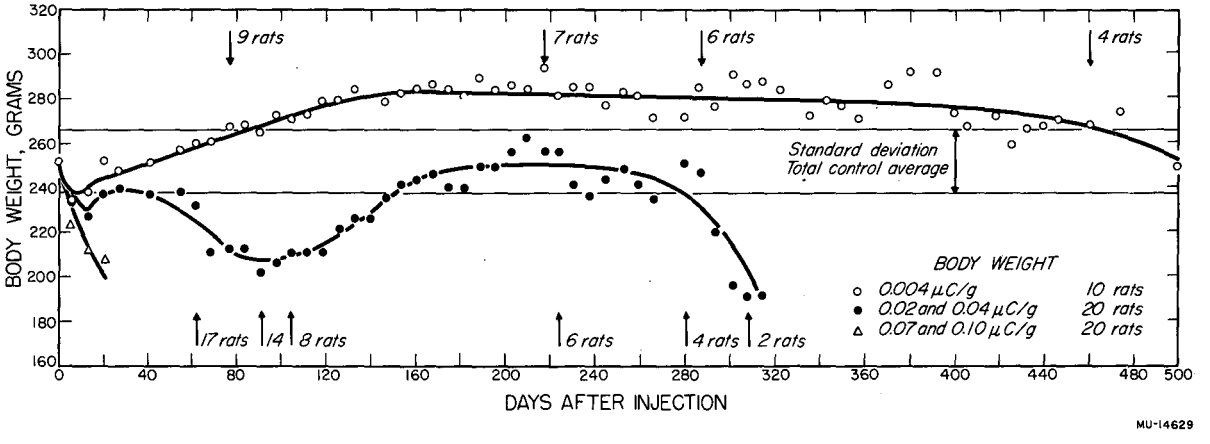

Fig. 16. The long-term effects of Ra^{223} on the body weight.

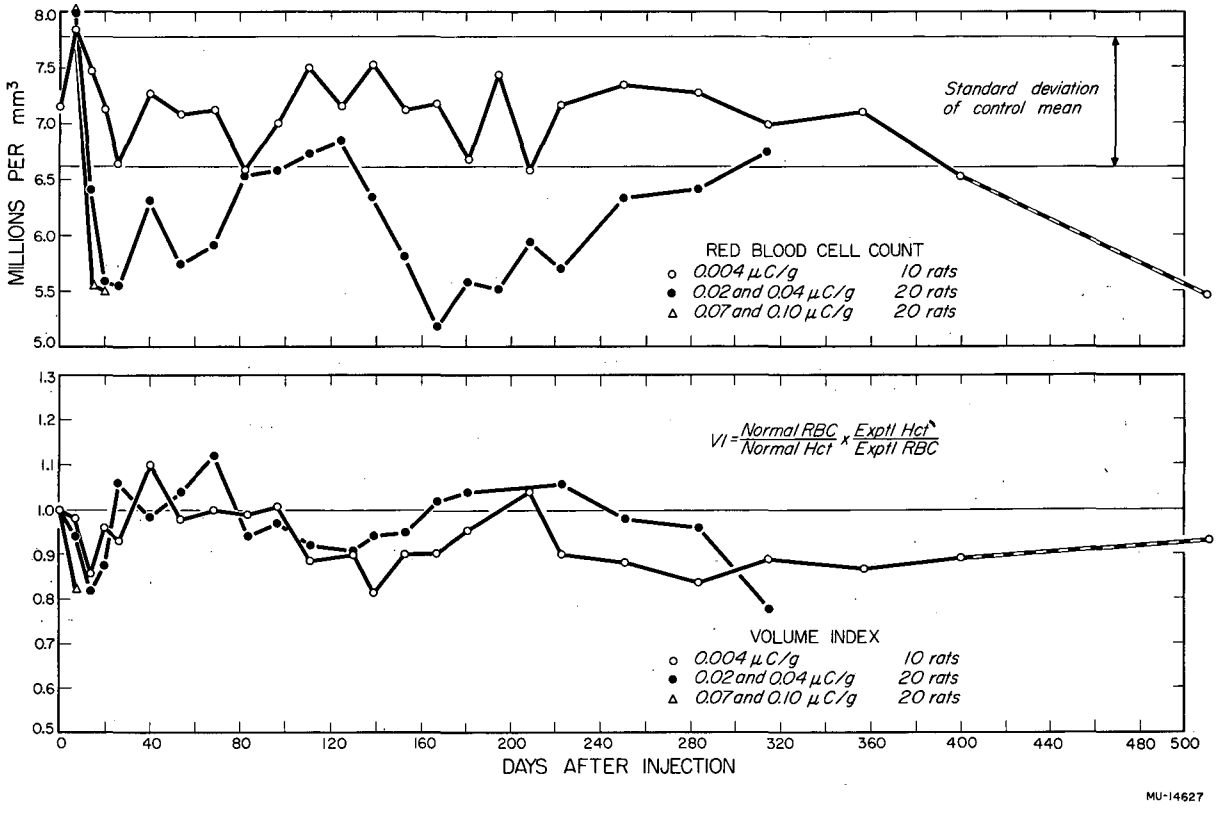

Fig. 17a(above). The long-term effects of Ra^{223} on the red blood cell count.

Fig. 17b(below). The long-term effects of Ra^{223} on the volume index of the red blood cells.

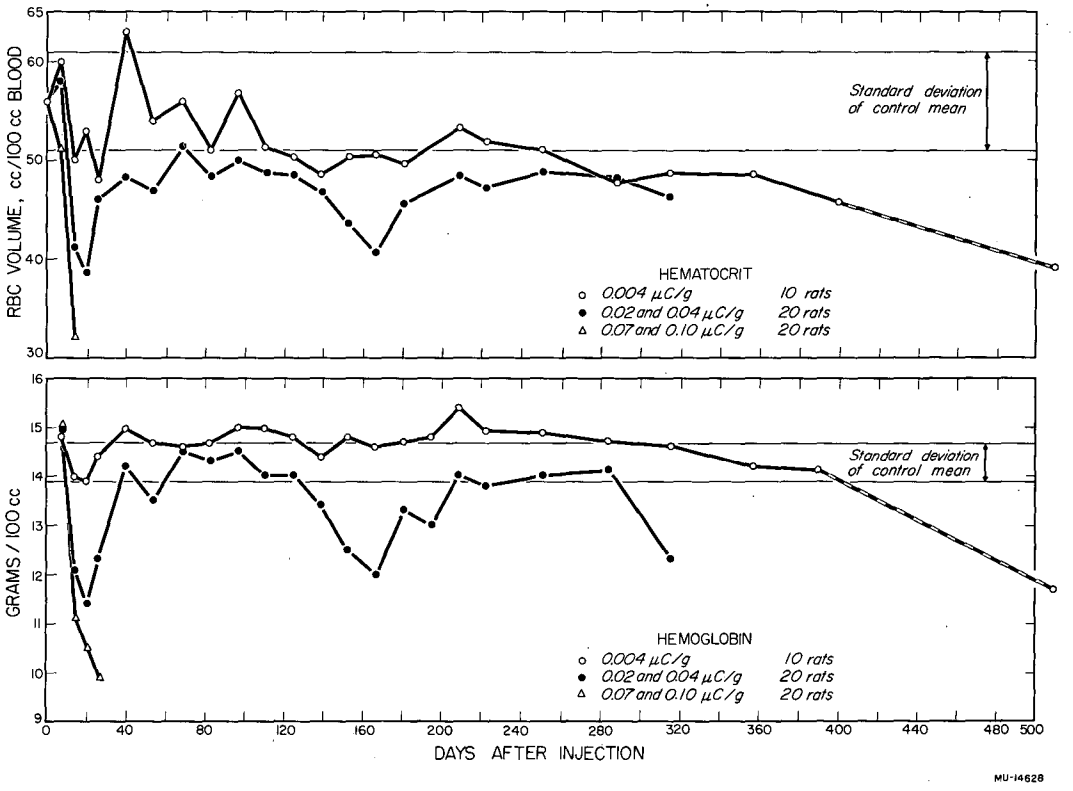

Fig. 18a(above). The long-term effects of Ra^{223} on the hematocrit.

Fig. 18b (below). The long-term effects of Ra^{223} on the hemoglobin level.

count of this group fluctuated about the normal mean. The hematocrit tended to be slightly below normal and the hemoglobin slightly greater than normal, resulting in a low volume index (Fig. 17b) and a nearly normal color index.

After an initial period of apparent hemoconcentration, the H, R, H, of the two highest-dosage groups, 0.07 μC/g and 0.10 μC/g, declined until death, reflecting the severely hemorrhagic condition of the animals and the aplastic state of the bone marrow (see section on acute pathology).

The sequence of events following a sublethal dose of Ra^{223}, 0.02 μC/g and 0.04 μC/g, was more complex than after either an acutely lethal dose or a relatively small dose. Subsequent to the initial rise, the H, R, H, fell below normal limits as a result of hemorrhage and marrow destruction, reaching a minimum on about the 20th day. During the next 80 days there was a trend towards recovery; the red cell count showed a net increase of 0.29% per day. A normal hematocrit was never achieved. It was exceedingly difficult to bleed the animals at these dose levels during this time (20th to 120th day after injection). The blood seemed abnormally viscous. It flowed very slowly, and clotted almost immediately upon withdrawal. No measurements were made of total red cell volume, but the characteristics of the blood samples strongly suggest some degree of hemoconcentration or a reduction in plasma volume. Either of these processes would result in high measured values for the H, R, H and lead to erroneous conclusions concerning the degree of hematopoietic recovery. From the 100th to the 160th day the erythropoietic elements suffered a second decline to about 75% of normal; the red cell count decreased at a rate of 0.69% per day, which is very nearly the same as the normal rate of red cell destruction.[18,19] It should be noted that the beginning of this second decline coincided with a period of highest death rate of these animals, and that bone marrow specimens taken during this time varied from sparsely cellular to almost aplastic. The survivors of this second wave of deaths showed a progressive recovery of the H, R, H so that they were close to the lower limit of normal by the 280th day. During this second recovery period the red cell count was increasing at the same rate, 0.29% per day, as it had during the initial recovery period shortly after the Ra^{223} injection.

The volume index (a rough measure of red cell size), and the measured red cell diameter shown in Figs. 18b and 19 agreed well. During the first three months after the Ra^{223} injection there was an excess of large cells in the circulation (presumably reticulocytes). For the remainder of the animals' lives the red cells were smaller than normal. The color index (not shown graphically) was nearly normal throughout the experiments for all 30-day survivors.

Chronic Effects on Lymphopoiesis and Granulocytopoiesis

The effect of Ra^{223} on the lymphocyte count is shown in Fig. 20a. Values for the highest-dosage groups were similar to those for the medium-dosage groups, and are not shown in the figure. As described in a previous section there was an early decrease in the white cell count exponentially related to dose for the entire range of Ra^{223} doses.

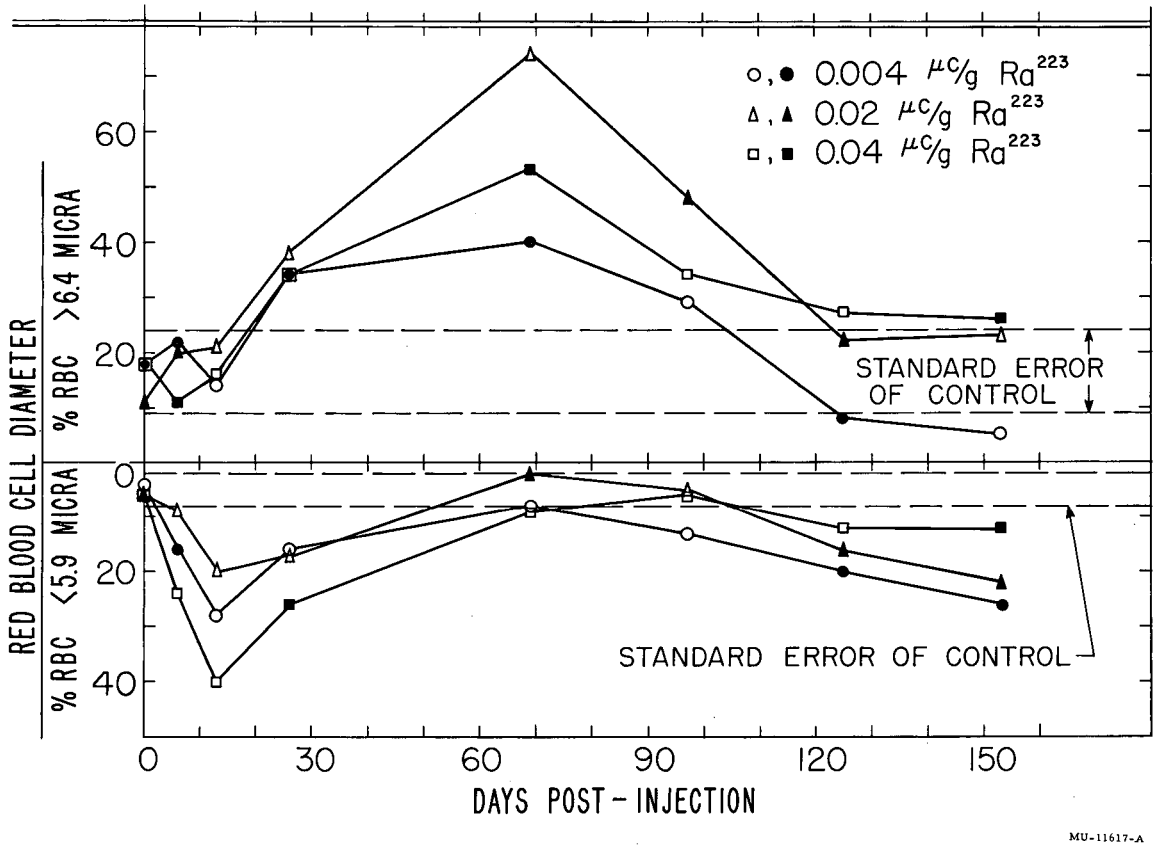

Fig. 19. The changes in red blood cell diameter as a function of time after injection of Ra^{223}.

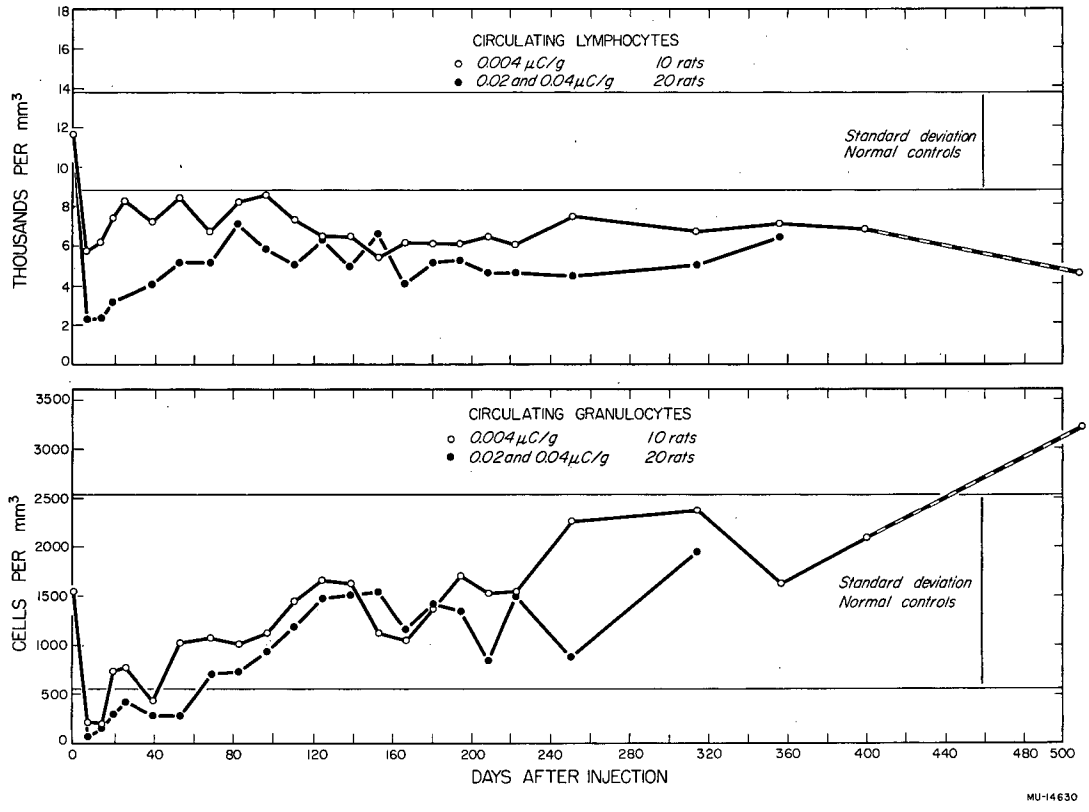

Fig. 20a(above). The long-term effects of Ra^{223} on the lymphocyte count of the peripheral blood.

Fig. 20b(below). The long-term effects of Ra^{223} on the granulocyte count in the circulating blood.

The initial recovery of lymphopoiesis was more pronounced at the medium than at the lowest dose; the groups, however, were indistinguishable by the 100th day. As indicated in Fig. 20a, recovery of lymphopoiesis was partial and only temporary. For the duration of the observation period, the lymphocyte count remained at about 50% of normal, the level to which the WBC of the lowest-dosage group had fallen immediately after the Ra^{223} injection. During the early stages of recovery and at all dose levels abnormal lymphocytes (large juvenile cells, poorly staining cells, cells that contained basophilic granules, or binucleated cells) were seen. After the 100th day these abnormal cells were found only occasionally, not always in the same animals or at any particular dose level.

The granulocyte count (eosinophilic and neutrophilic leukocytes) is shown in Fig. 20b. The granulocytes were markedly depressed very shortely after the Ra^{223} injection, and at the higher doses these cells were only rarely seen in the stained smears. The 30-day survivors at all doses had granulocyte counts within the normal limits by the 100th day, and except for a few scattered points, differences between the various dosage groups were insignificant.

It is interesting to compare the recovery of granulocytopoiesis with that of erythrocytopoiesis (Fig. 17a). The time lag of the early decline in the red cell count (20 to 30 days) compared with that of the granulocytes (7 to 14 days) reflects the longer life span of the red cells.[18] At the lowest dosage level the number of circulating marrow-produced cells was within the normal range for each cell type by the 100th day. At the medium dose levels, however, although recovery of granulocyte count appeared to be both permanent and complete, achievement of a nearly normal erythrocyte count was only temporary and was followed by a second decline and a return to low normal only shortly before the death of the longest-term survivors.

Long-Term Histological Findings

Complete autopsies were performed on nearly half the long-term survivors. The numbers of animals, the dose levels, and the time after injection are given in Table V. As shown in the table, femurs were available from a previously unreported series of experiments in addition to the specimens from this mortality series. Age controls were available for all except the very oldest long-term survivors.

Thyroid

No alterations were seen in the thyroid gland other than those attributable to normal aging.[20]

Ovary and Uterus

At the 0.04-μC/g level these tissues appeared somewhat hypoactive; otherwise, only age-related changes were observed.

Adrenal

In the specimens taken 125 days postinjection (from all but the lowest-dosage group), the adrenal cortex was notably thinned, the fasciculata was disorganized, and the blood vessels in the glomerulosa were widely dilated. At the later times these glands were within normal limits.

Table V

Number of Ra^{223} femur specimens and the ages of the animals from which they were taken

Dose level (μC/g)	No. rats	Days postinjection	Chronologic age (days)
Normal controls	5	---	275
0.004	2	200	310
0.004	4	500	610
0.02	2	125	235
0.02	2	200	310
0.02	2	300	410
0.04	2	125	235
Femurs only			
0.008	7	210	300
0.017	8	210	300
0.03	2	156	250
0.054	6	156	250

Lung

Pneumonitis was found in varying degrees, but neither the incidence nor the extent of involvement bore any apparent relationship to dose level or time after injection. Occasional deposits of golden-brown pigment were seen which were probably the remnants of old hemorrhages.

Kidney

At the higher dose levels, prior to 200 days, mild tubular degeneration was seen and avascular or fibrotic glomeruli were relatively common. At the later times the kidneys were generally normal for all dosage levels examined. The only observable changes were scattered deposits of pigment and an occasional scarred glomerulus, suggesting previous spotty damage.

Liver

In the earlier specimens at the higher dose levels the livers showed cloudy swelling, often nearly occluding the sinusoids. Some fibrotic patches were seen in the neighborhood of the portal spaces. The 200-day specimens still showed some cloudy swelling, enlarged blood vessels, and occasionally moderate central necrosis. The livers of the very-long-term survivors were normal except for a few scattered islands of necrotic cells and occasional areas of bile-duct proliferation.

Thymus

At the earlier times the lymphatic tissue was depleted and was being replaced by fibrous tissue and embryonic fat. After the 200th day it was difficult to differentiate between unrepaired damage and the normal thymic involution that occurs in older animals.

Lymph nodes

Generally the nesenteric nodes appeared more serously damaged than those from the cervical region or axilla (see section on acute pathology). At all times, and particularly above the 0.02-μC/g level, the lymph nodes were almost exhausted; the cortex was very thin, the sinusoids were dilated, there were few germinal centers, and the connective-tissue framework was conspicuous. Macrophages containing pigment were common. The 500-day specimens from the lowest dose level were the same as described above although perhaps to a lesser degree. Whereas the follicles themselves seemed intact, the frame-work was obvious, and the germinal centers that were present were hypoplastic.

Spleen

In the 125- and 200-day specimens at the 0.02-μC/g and 0.04-μC/g levels the white pulp was markedly depleted, and the red pulp was filled with macrophages containing golden-brown pigment. One specimen contained small ectopic sites of myelopoiesis. The 300- to 500-day specimens from the 0.004-μC/g and 0.02-μC/g groups showed white pulp that was still very depressed, with little evidence of lymphopoiesis. The framework was conspicuous, the follicles small, and germinal centers rare. Ectopic

hematopoietic activity was seen in varying degrees in the four specimens taken at 500 days, and ranged from a few foci of megakaryocyte formation to a completely myelopoietic spleen. In the latter, normoblasts and juvenile eosinophils were easily identified.

Bone Marrow

The degree of recovery of the marrow was roughly inversely proportional to the Ra^{223} dose. At the highest Ra^{223} level for which there were long-term survivors, 0.04 μC/g, the marrow in the 8-day femur specimens was severely damaged (see Fig. 24). In the epiphysis and immediately below the epiphyseal plate the small marrow pockets were empty except for islands of red cells suspended in an eosinophilic, fibrinous coagulum. Deeper in the shaft variable quantities of cellular marrow remained, usually located directly in the center of the shaft. The nuclei of many of these surviving cells were pyknotic, and the number of viable cells was reduced. By the 125th day the marrow in the ribs and vertebrae was only sparsely cellular, and that deep in the femoral shaft seemed nearly normal; however, the metaphysis and the epiphysis still contained gelatinous marrow.

The acute specimens at the next lower dose level, 0.02 μC/g, were similar to the above group except that the aplasia deep in the femur shaft was not nearly as marked. The two 125-day specimens showed almost aplastic marrow in the vertebrae and ribs and occasional islands of normal cellular marrow in the femoral epiphysis and normal cellularity deep in the shaft, but no significant repopulation in the metaphysis near the bony trabeculae. The cellularity of the marrow in the ribs and vertebrae of the four specimens taken between the 200th and the 300th day was generally improved except near the cartilage plates. Repopulation of the femoral epiphysis appeared nearly complete (see Fig. 30), but the metaphyseal region was still nearly empty of marrow. Deep in the shaft the marrow of one specimen contained almost no adipose elements and appeared hyperplastic.

At the lowest dose level, 0.004 μC/g, 8 days after the Ra^{223} administration, the marrow was generally hypoplastic (as is seen in Fig. 23), but not so much so as at higher dosages. The metaphysis was the most depleted region. Deep in the shaft the marrow was still predominantly cellular, and the majority of the cells appeared viable. By the 200th day recovery of the marrow in this group was well under way (Fig. 27), and in contrast to the higher-dosage specimens obtained at this time, the epiphysis and metaphysis were uniformly repopulated. Of the four 500-day specimens (Fig. 28) two were within normal limits for old rats; the marrow of the other two was hyperplastic. Myelogenous leukemia was diagnosed in one of the 500-day animals (Rat 465). The pertinent data are shown in Table VI.

Bones

Vertebrae, ribs, and mandibles were examined from animals in the main toxicity series up to the 300th day. The changes seen in the vertebrae and ribs were generally similar to those described below for the femurs. In the mandibles, the incisor root was anchored very poorly, if at all. The connective tissue lining the socket was inflamed and sometimes edematous. The number of odontoblasts was definitely decreased. By the 300th day a basophilic lamina

Table VI

Measurements of circulating blood and bone marrow of rats surviving 500 days after 0.004 μC/g of Ra^{223}.

	Rat number			
	456	503	465	480
Total white count[a]	5900	4950	14,050	6600
Granulocytes	2750	1490	6100	3530
Lymphocytes	3150	3460	7950	3070
Red cell count[a]	4.5×10^6[b]	7.36×10^6	4.29×10^6[b]	5.63×10^6
Myeloid to erythroid ratio (marrow)[c]	1.12	1.43	4.9	4.0
Histologic appearance of marrow	hyper-plastic	normal	hyper-plastic	normal
Appearance of spleen (Ectopic myelo-poiesis)	rare foci	rare foci	entirely myelo-poietic	moderately myelo-poietic

[a] Cell counts in number of cells per mm^3.

[b] Large numbers of basophilic RBC in stained blood smear.

[c] Normal M/E rates for 400-day old rats is 2.99.

had replaced the odontoblast layer. The poor attachment of the incisor roots and the impaired growth mechanism were reflected grossly in the lower incisor teeth, which were badly worn and spread apart.

The effect of Ra^{223} on bone growth was best seen in the distal end of the femur. Because the greatest number of specimens was obtained on the 8th and 200th days postinjection, the description of anatomical changes effected by increasing Ra^{223} dosages refers for the most part to these times.

In general, the effects of a single injection of Ra^{223} on the bone of the 100- to 120-day-old female rat were similar to those described by Heller[21] for adult mice given Sr^{89}.

The epiphyseal plate shown in Figs. 21 and 22 and the subjacent primary and secondary spongiosa were characteristic of normal slowly growing bone. The histological features closely resembled those described for rats of this sex and age in a neighboring region--the proximal tibia epiphysis--by Becks, Simpson and Evans.[22]

At the lowest Ra^{223} level, 0.004 μC/g, 8 days after the injection, the cells and matrix of the epiphyseal plate were within normal limits (Fig. 23). Isolated, rounded dying cartilage cells were occasionally found. The increased plate width (Table VII) resulted from an increase in the width of the region of enlarged vacuolated cells. Although some vascular tufts from the marrow still impinged upon this vacuolated region, their number was reduced, and they were farther apart, leaving areas where cartilage erosion was in abeyance. In such regions new bony trabeculae were sparse, and the beginnings of the "severance" described by Heller[21] could be seen. Deeper, towards the diaphysis, fragments of the primary spongiosa persisted and an abundant anastamosing secondary spongiosa was seen. The osteoblasts on these bony surfaces were for the most part flat and fusiform (the so-called spindle cells of Heller).[21] Osteoclasts were sparse but still present. A thin basophilic line was observed on the surfaces of many of the trabeculae beneath the osteoblastic layer.

In the cartilage plates of the acute specimens of the 0.02-μC/g group the region of proliferating chondrocytes contained rows of spherical rather than flattened cells. The acidophilic cytoplasm and pyknotic nuclei of these cells indicated cell death. The vacuolated zone was substantially broadened through nonremoval of enlarging chondrocytes. Often where cartilage had recently been incorporated into primary spongiosa, the new bony trabeculae contained cartilage remnants involving several lacunae, some of which still contained dead cartilage cells. The marrow immediately below the cartilage plate was aplastic and avascular. Broad areas of "severance" were found. Where seen, the osteoblasts were spindle-shaped cells. No osteoclasts were observed in the neighborhood of the epiphyseal plate.

The histology of the acute specimens at the 0.04 μC/g level (Fig. 24) closely resembled that of the 0.02-μC/g group. More of the isolated, rounded clusters of necrotic cartilage cells were seen in the epiphyseal plate, and these cells were surrounded by larger amounts of a somewhat more fibrous matrix. The over-all irregular widening of the plate due to persistence of vacuolated cartilage cells was further increased beyond the 0.02-μC/g group.

ZN-1955

Fig. 21. Distal femur of a normal 110-day-old female rat. H and E, X 23.

ZN-1944

Fig. 22. Distal femur of a normal 110-day-old female rat. H and E, X 42.5.

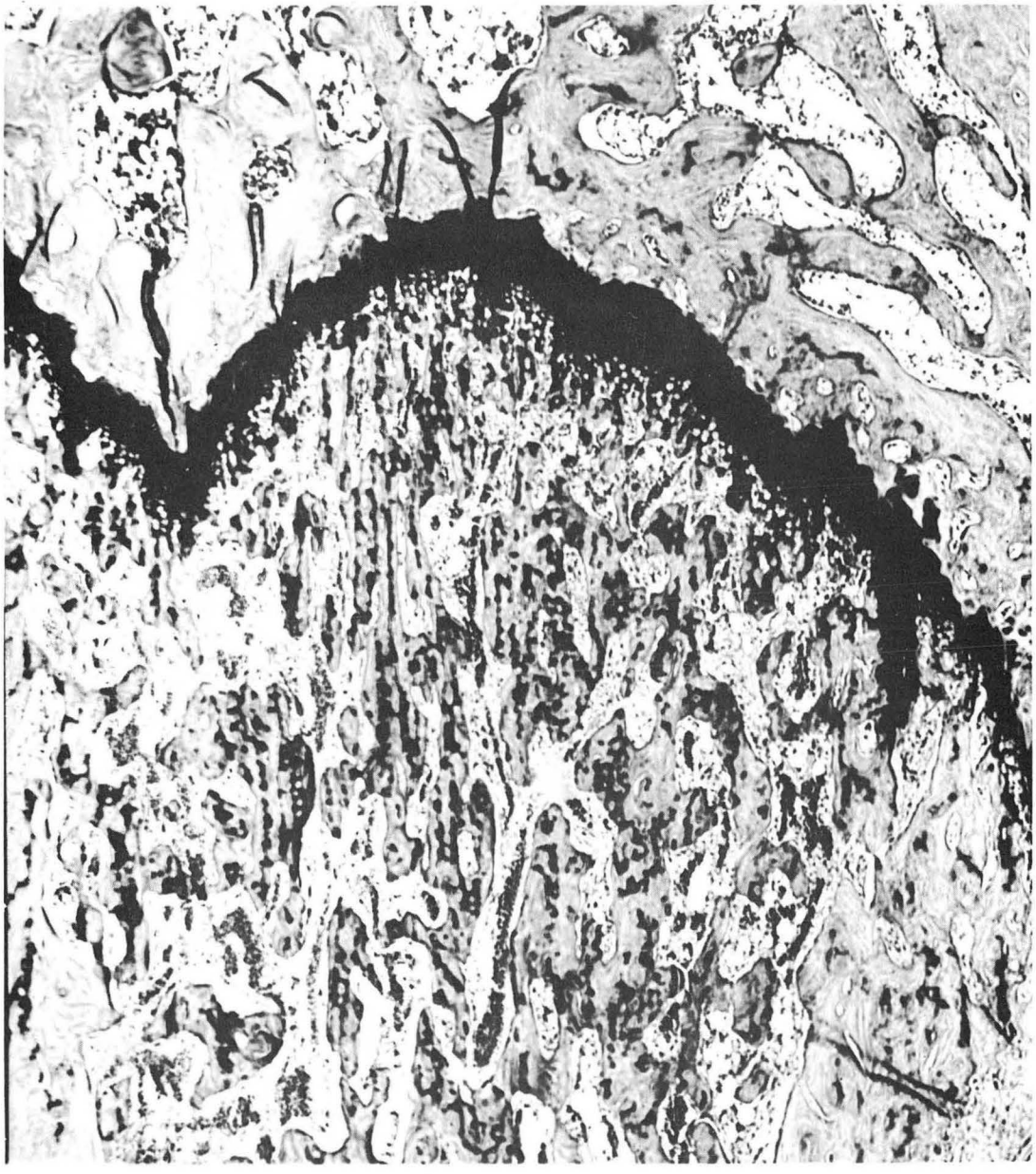

ZN-1945

Fig. 23. Portion of the epiphyseal plate of the distal femur of a 110-day-old rat, 8 days after receiving 0.004 μC/g of Ra^{223}. H and E, X42.5.

Table VII

The effects of various levels of administration of Ra^{223} on the width of the epiphyseal plate of the distal end of the femur. The animals were female rats 120 days of age that were sacrificed 8 days after the Ra^{223} injection.

Ra^{223} dose (μC/g)	No. of femurs	Plate width (microns ± S. E.)[a]
Control	5	70 ± 4.9
0.004	5	94 ± 5.7[b]
0.02	5	131 ± 6.1
0.04	6	148 ± 7.6
0.07	8	145 ± 8.0
0.10	7	126 ± 7.6

[a]Plate width was measured in the same three places on each specimen, so that the group mean was determined for three times the actual number of femurs.

[b]Underlined means were compared with the mean directly above by the t-test of Fisher, and the P value was beyond the 1% level of confidence. All experimental group means were significantly different from the control mean ($P < 0.01$).

ZN-1946

Fig. 24. Portion of the epiphyseal plate of the distal femur of a 110-day-old rat, 8 days after receiving 0.04 μC/g of Ra^{223}. H and E, X 42.5

Eight days after injection of 0.07 μC/g of Ra^{223}, the cartilage plate showed large areas where all cartilage-cell alignment was lost in the proliferative zone (Fig. 25). The cells in these regions of disorganization were dead, and the matrix surrounding them was degenerating. Irregularities in plate width were more pronounced than in the preceding group; however, the width of the vacuolated zone was nearly the same as at the 0.04-μC/g level. The incidence of "severance" of the epiphyseal cartilage from the primary spongiosa was very much less than in the two preceding groups. In this group a phenomenon that had been seen sporadically (and only to a minor degree) in the preceding groups became pronounced, i.e., a marked erosion and undercutting of the bone on the dorsal aspect of the metaphysis just under the margin of the epiphyseal plate. Numerous osteoclasts were associated with this bone resorption. From the periosteum substantial masses of fibrous tissue had invaded the space created by this bone removal, and the resorption cavity, which continued down the shaft, had been filled with a material resembling fibrocartilaginous callus. The pleomorphism of this connective tissue is reminiscent of that found by Owen[23] in a similar anatomical position in the tibias of rabbits given radiostrontium. Although in these acute Ra^{223} bones (as also in Owen's acute Sr^{90} specimens) the fibrous replacement tissue is not malignant, this is the site at which she later found malignant bone tumors.

The femurs taken from animals receiving the highest dose of Ra^{223}, 0.10 μC/g, were for the most part similar to those of the preceding group. The cartilage plate seemed somewhat narrower, although marked irregularities in its width prevented statistical demonstration of a difference. The majority of the cartilage cells were dead or dying. Whereas, in preceding groups, an excess of vacuolated cartilage cells was seen, this excess was less conspicuous at the highest dose level. It may be that proliferation of the cartilage cells was suppressed more abruptly and that fewer cells were able to mature and enlarge.

In the 300-day-old controls (Fig. 26) there was still evidence of slight growth with cartilage proliferation, erosion by marrow tufts, and the formation of some small primary trabeculae. As is usually seen in older rats, the cartilage matrix on the diaphyseal side of the epiphyseal plate tended to be basophilic rather than eosinophilic as it is in the proliferating zone. A few small islands of abnormal cartilage, and a few segments of sealing bone were seen. For a more complete histological description, see Becks, Simpson, and Evans.[22]

Specimens were available at the lowest Ra^{223} injection level at 200 and 500 days. By the 200th day the cartilage plate was very narrow; in one case it was unrecognizable (Fig. 27). The cartilage was sealed off from the marrow cavity by a dense lamina of bone. There was little or no new primary spongiosa. There were few changes from the foregoing in the next 300 days except that the metaphyseal trabeculae had undergone further resorption (Fig. 28). The few bony trabeculae present were very deep in the marrow cavity and often contained an abundance of matrix and occasional cores of necrotic cartilage. These trabeculae resembled primary spongiosa and were sometimes arranged as a continuous bony bar parallel to the epiphyseal plate. At this dose level bone growth was markedly retarded soon after the irradiation, and then ceased at an earlier age than in normal animals.

ZN-1947

Fig. 25. Portion of the epiphyseal plate of the distal femur of a 110-day-old rat, 8 days after receiving 0.07 μC/g of Ra^{223}. H and E, X 42.5.

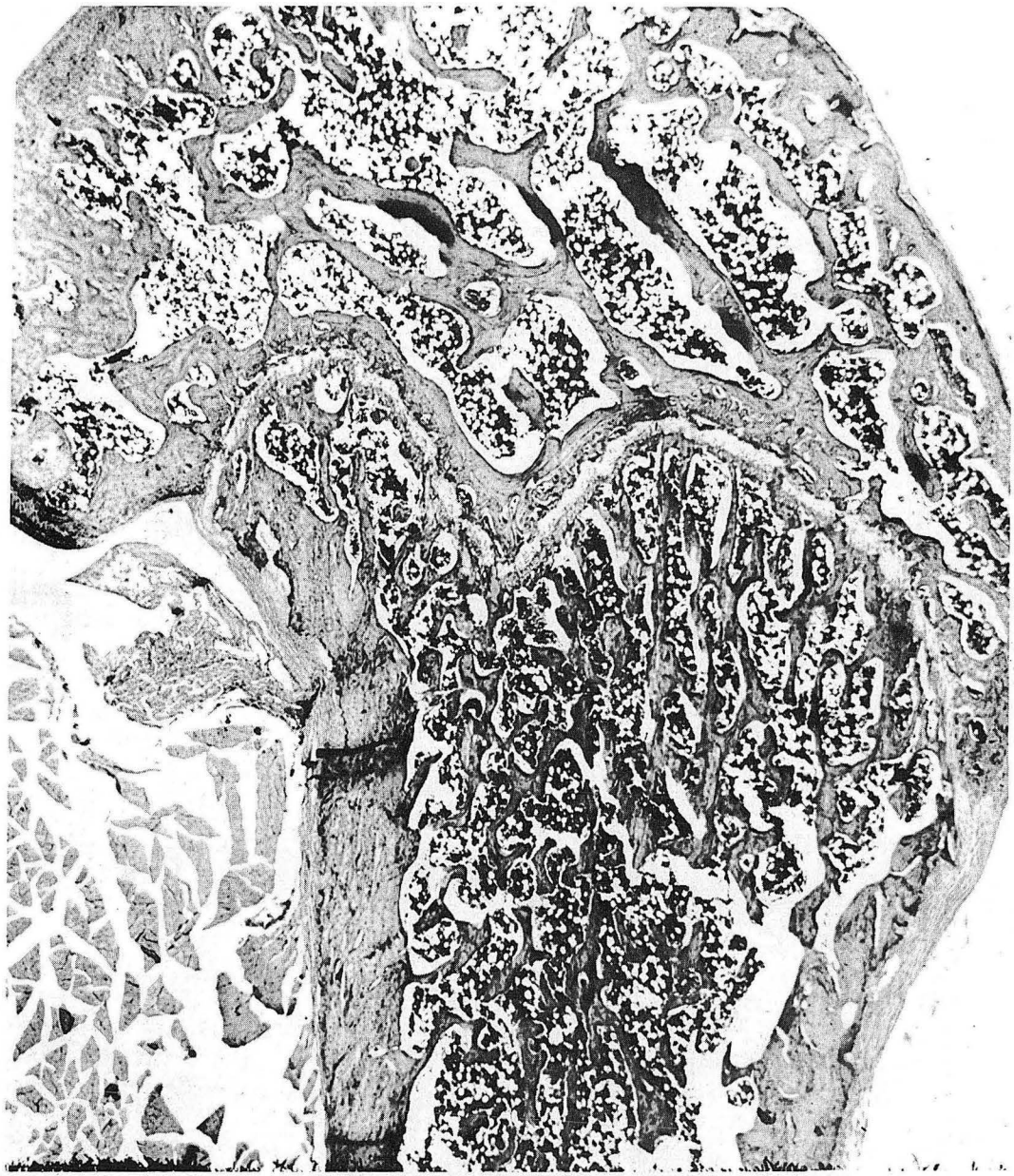

ZN-1948

Fig. 26. Distal femur of a normal 300-day-old rat. H and E, X 23.

Two hundred days after a Ra^{223} injection of 0.008 μC/g the epiphyseal plate was narrow, and occasionally it had been completely resorbed with epiphyseal-diaphyseal union (Fig. 29). When present, the chondrocytes were single or occurred in clumps or nests of cells, and only rarely occurred in columns. The remnants of the plate were generally separated from the marrow cavity by a transverse lamina of sealing bone. Deeper in the marrow cavity there was a broad, almost solid mass of "sworls" of bone. This bony mass consisted of trabeculae of primary spongiosa, most of whose lacunae were empty or contained dead osteocytes and spicules of unremodeled cartilage matrix. The bony trabeculae and the cartilage spicules were surrounded by and embedded in thick strands of fibro-osseous material. Between this mass and the epiphyseal plate there was occasionally remnants of earlier epiphyseal cartilage, and, in one case, almost a second plate. The lacunae of this older cartilage were very large, and the cells were degenerate. There was no evidence that growth was progressing at the time the specimens were taken, but the distance between the true plate and the heavy bar of bone apparently represented a period of growth following the initial radiation damage.

Specimens were available 125 to 300 days after administration of 0.02 μC/g of Ra^{223}. There were few, if any, differences between the histological features of the earlier and later specimens. In most the cartilage plate was very wide and highly disorganized (Fig. 30). For the most part the cells in the plate were degenerate and occupied rather large lacunae. There was little of the orderly proliferation and vacuolation associated with growth. About one-half the disphyseal side of the plate continued immediately into a heavy bar of bone which extended deep into the marrow cavity. The histology of this bony barrier was just like that described for the preceding group. In restricted regions of most of the specimens the marrow had penetrated the bony barrier, and partial separation of the epiphyseal plate and barrier was seen. That portion of the cartilage in contact with the bony barrier was necrotic, whereas in the portion toward the epiphysis (the remainder of the true plate) there were some small nests of apparently viable cells.

Animals receiving the higher doses, 0.03 to 0.05 μC/g, of Ra^{223} formed a more or less homogeneous group as regards their histology (Figs. 31 and 32); however, the pathological changes were somewhat more pronounced at the very highest doses. Generally the cartilage plate was very wide. On the epiphyseal side there were a few scattered rounded large chondrocytes. Towards the diaphysis the chondrocytes were arranged in very long orderly columns, which at first glance resembled those of actively growing young bone. However, they either were empty or were occupied by dead cells. Immediately subjacent to the columns of dead chondrocytes there was a bony barrier somewhat like that seen in the two preceding groups, but in which bone itself was more sparse, and although fibroblasts were rare, the intervening sworls were fibrous rather than fibro-osseous. Thus the bony bar was neither so dense as at the lower dose levels nor was it so wide, indicating a very rapid growth arrest. Even at these high levels occasional marrow tufts had managed to interpose between the cartilage and the bony barrier, creating small restricted regions of "severance."

ZN-1949

Fig. 27. Distal femur of a 300-day-old rat, 200 days after receiving 0.004 μC/g of Ra^{223}. Giemsa, X 23.

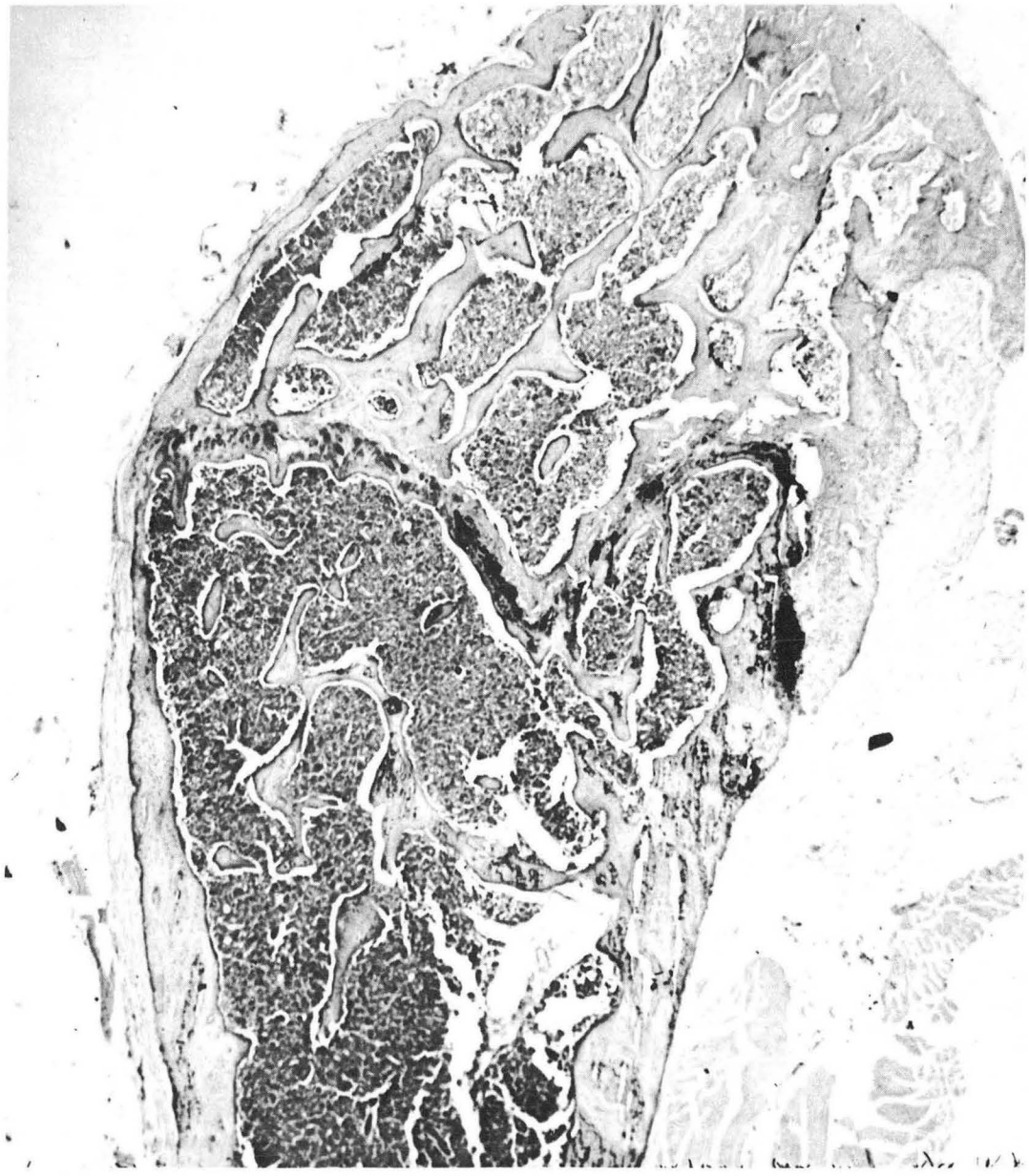

ZN-1950

Fig. 28. Distal femur of a 600-day-old rat, 500 days after receiving 0.004 μC/g of Ra^{223}. H and E, X 23.

ZN-1951

Fig. 29. Distal femur of a 300-day-old rat, 200 days after receiving 0.008 μC/g of Ra^{223}. H and E, X 23.

ZN-1952

Fig. 30. Distal femur of a 300-day-old rat, 200 days after receiving 0.017 μC/g of Ra^{223}. H and E, X 23.

ZN-1953

Fig. 31. Distal femur of a 300-day-old rat, 200 days after receiving 0.03μC/g of Ra^{223}. H and E, X 23.

ZN-1954

Fig. 32. Distal femur of a 300-day-old rat, 200 days after receiving 0.054 μC/g of Ra^{223}. H and E, X 23.

DISCUSSION

At dosage levels of the order of 1 μC per rat, Ra^{223} was more rapidly eliminated than are the lighter alkaline earth elements. Skeletal retention curves for the three radioelements, Ca^{45}, Sr^{90}, and Ra^{223} in adult female rats are as follows:

$$= 4.4\% e^{-0.693 t/2} + 6\% e^{-0.693 t/6} + 67\% e^{-0.693 t/570}, \quad (15)$$

$$= 7\% e^{-0.693 t/2} + 12\% e^{-0.693 t/12} + 43\% e^{-0.693 t/570}, \quad (16)$$

$$= 18\% e^{-0.693 t/1.6} + 40.5\% e^{-0.693 t/76}, \quad (17)$$

where t is the time in days after a single intramuscular injection.

The initial rapid components in the above equations are presumed to represent the fraction of each isotope deposited on bone mineral surface that is readily exchangeable with blood-borne calcium. A larger portion of Ra^{223} than of Ca^{45} or Sr^{90} was eliminated promptly from the skeleton (the coefficient of the first term in Eq. (17) and with a somewhat shorter half time. These observations suggest that Ra^{223} in an alkaline earth position on the surface of a crystal of bone salt is relatively unstable with respect to replacement by a smaller calcium ion.

Although skeletal retention of Ca^{45} and Sr^{90} was determined over an 8-month period, the short physical half life of Ra^{223} limited the observation period for it to the first 60 days after injection. A slow component of the retention curve comparable to that found for Ca^{45} and Sr^{90} would probably not have been observed for Ra^{223} even if more extended measurements had been feasible. As was pointed out in the section dealing with skeletal pathology, even the 0.004-μC/g dosage employed as a "tracer" drastically altered bone growth. Formation of new bone was markedly reduced with premature sealing of the epiphyseal plate by bone. The sparseness of trabeculae in the metaphysis of the femur after long postinjection intervals indicated that bone resorption was probably only partially impaired at this dose level. Continued resorption without normal renewal processes resulted in a relatively rapid elimination of skeletally deposited Ra^{223}. Hence, the histo-physiologic mechanisms for an extended retention component representing gross structural bone turnover are lacking.

At Ra^{223} levels greater than 0.02 μC/g elimination from the skeleton was retarded, and the percentage of radium retained was dependent upon the amount administered. At these levels bone growth ceased abruptly and resorption was noticeably impaired. At very high dosages both proliferation and resportion ceased. Failure of the resorptive mechanism following intense irradiation from large amounts of Ra^{223} provides a partial explanation of the prolonged half time for its elimination from the skeleton (173 days at 0.04 μC/g contrasted to 76 days at 0.04 μC/g) and of the observed dose dependence of skeletal radium retention.

In the rat the form of the alkaline earth excretion curve seems to be determined in part by the degree of skeletal radiation damage. At moderate

radiation levels, as long as the skeletal vasculature remains intact, and resorption and remodeling of bone proceed to some extent, the elimination curve is a series of several exponentials. At high dosages, at which radiation damage significantly alters the gross turnover of bone, the excretion curve is better described by a single-power function (see Norris and Evans[5]).

The pattern of acute mortality following the administration of Ra^{223} suggested a single mode of irradiation death. Severe hemorrhage, as indicated by gross and microscopic pathology, was the most probable cause of death during the first 21 days. It should be pointed out that this isotope provides a unique method for the study of acute effects of densely ionizing radiation on the mammalian skeleton and hematopoietic tissues uncomplicated by gastrointestinal symptoms or massive destruction of lymphatic tissues.

The irregular geometrical pattern of radiation from alpha-particle emitters that are deposited primarily on bony surfaces presents some difficult problems in the interpretation of radiation effects in the bone marrow. Histological sections of bone reveal regions of marrow that have received lethal amounts of radiation and are largely acellular. In the same sections a short distance from the bone surfaces (beyond the particle range) other marrow volumes can be found that have received little or no radiation and appear to be normally cellular. Under these circumstances one would expect curves relating the functional state of the marrow and radiation dose to show initial radiation-sensitive components followed by a "tail" of constant value representing normal function of the surviving marrow. This was not the case, and the curves of Fe^{59} uptake in the red cells and of the granulocyte count (shown in Fig. 15) included at least one additional component of moderate slope. The complexity of these curves implies the participation of other less radiation-sensitive processes than marrow destruction. In our judgment impairment of the general nutritional status of the Ra^{223}-injected rats and "starvation" of the unirradiated marrow due to radiation damage of the skeletal vasculature are likely contributors to the progressive decline observed in marrow function as the Ra^{223} dose was increased.

It was apparent that the nutritional state was poor in the higher Ra^{223} dosage groups, 0.04 to 0.10 μC/g. At these dosages animals sacrificed at 8 days showed specific tissue wasting, loss of internal fat, and an average body weight loss of 35 g. Disturbed liver cytology varying from cloudy swelling to hydropic degeneration strongly suggested at least partial loss of hepatic synthetic activity.

Looney[25] and Owen et al.[23] have indicated that vascular damage may play a major role in the pathological skeletal changes that follow deposition of radioactive alkaline earths. It is entirely possible that disturbance of the circulation in those bones that contain marrow may have a profound effect on the marrow as well.

The blood supply of bones has been described by Weinmann and Sicher[26] and is illustrated by Maximow and Bloom[27] and by deMarneffe.[28] The blood supply of spongy bone is represented by the blood vessels of the marrow spaces, which are generally equidistant from the surrounding bony trabeculae. In the compact bone the blood vessels, primarily capillaries, occupy the network

of the longitudinal Haversian and connecting Volkmann's canals. Volkmann's canals contain not only the transverse links of the capillary network, but also arterioles and venules for the connection of the periosteal vessels with the medullary vessels of the bone.

Examination of the blood supply of the long bones is of particular interest in that the femur made up the bulk of the bone specimens examined in these experiments. The femur shaft is supplied from three sources, the nutrient artery, the metaphyseal arteries, and the periosteal arteries. As long as the epiphyseal cartilage persists, the epiphysis has an independent blood supply originating from the capsular arteries. The nutrient artery penetrates the compact bone and, in the marrow cavity, splits into an ascending and a descending branch. After supplying the marrow these send terminal branches into the metaphysis where they anastamose with the metaphyseal arteries. The latter are derived from the muscles and ligaments and enter the metaphysis around its circumference. The metaphyseal capillary network ends toward the epiphyseal cartilage in long hairpin-shaped loops. In addition to the nutrient and metaphyseal artieres, the compact bone receives many small periosteal artieries which enter the Volkmann canals. Although mainly supplying the compact bone, they anastamose with the arterioles of the metaphysis. The veins of a bone follow the arteries, beginning with wide venous capillaries into which the arterial capillaries open abruptly.

One can then picture a vascular system that is dependent upon many small anastamosing vessels for optimal free flow. In the long bones, most of the transition from arterial to venous circulation appears to occur in the metaphysis, where active calcification is taking place. Thus those vessels close to the epiphyseal plate, those running close to trabecular surfaces, those entering the marrow cavity from the Volkmann's canals at the endosteal surface, and the small vessels in the compacta that are completely surrounded by bone can be subjected to intense radiation from radium deposited on the bony surfaces adjacent to them. Femur sections from the high-dose animals (0.07 and 0.10 μC/g) sacrificed at 8 days showed many vascular spaces in these regions that were empty of blood cells, other vessels that were collapsed, and still others that were filled with an amorphous coagulum. There was no detectable capillary network in the epiphysis or in the metaphysis below the epiphyseal cartilage. In the femur shaft and the marrow spaces of the vertebrae the sinusoids were often widely dilated, indicating stasis--an observation that is not too surprising when one considers that much of the main capillary network joining the arterial and venous circulations had been destroyed.

Vascular lesions have been observed in the lymph nodes of rabbits after 2,000 to 3,000 r of locally applied x-ray and in the skin of rodents exposed to external sources of beta radiation.[29] In the 8-day Ra^{223} femur specimens, vascular damage was noted in areas other than immediately adjacent to the epiphyseal plate, occasionally at the 0.04μC/g level and frequently at the two higher dosages. It was calculated (see Appendix) that in 8 days a Ra^{223} dosage of 0.04 μC/g would deliver approximately 1850 rad to the marrow and the epiphyseal plate. This dosage is of the same order of magnitude as x-ray and beta dosages required to produce slowly healing vascular lesions.

The presence of skeletal vascular lesions may also help to explain the pattern of marrow repopulation in the heavily irradiated parts of the bones and the slowness of this recovery process. In the femur, the metaphyseal marrow was invariably the hardest hit and was the last region to be repopulated by cellular marrow. After receiving a mean lethal dose of whole-body radiation (600 to 800 r, which does not damage the vasculature or the primitive reticular stem cells to any great extent), recovery of the marrow of laboratory rodents proceeds almost uniformly throughout the marrow cavities and is nearly complete 40 days later.[30] In contrast, because of its uneven distribution pattern in bone, the radiation from Ra^{223} was sufficiently intense in some regions to destroy the primitive reticular cells and the vascular bed as well as the differentiated myeloid cells. Consequently, the only means by which marrow production could be re-established in these regions was the relatively slow process of vascular proliferation and migration of myeloid elements from the less damaged regions.

The large discrepancy between the measured toxicities of Ra^{223} and natural radium, Ra^{226}, in laboratory rodents is also worth mention. Fink and his co-workers report a mean lethal dose at 30 days (LD_{50}/30 days) of 1.6 μC/g of Ra^{226} in adult male and female Wistar rats.[31] The LD_{50}/30 days for adult mice and Sprague-Dawley rats was estimated as 1 μC/g by Bloom's group.[32] Our measured toxicity for Ra^{223} was close to 0.05 μC/g. It would appear then that Ra^{223} is 20 to 30 times as toxic as natural radium. It can be seen from the Appendix that at a Ra^{223} dosage of 0.05 μC/g the skeleton accumulates about 4,000 rad in 30 days, and of this 65% (2,600 rad) is absorbed in the first 10 days. According to our calculations the quantity of Ra^{226} (aerated to remove the radon daughter initially) that delivers 2,600 rad to the skeleton in 10 days is 0.172 μC/g. On a per-microcurie basis Ra^{223} should be about 3.5 times as toxic as Ra^{226}.

The rate of dose delivery is not the same for these two isotopes. The importance of dose rate is pointed up by the recent work of Grahn et al., who have exposed mice continually to Co^{60} γ-radiation, and have found that doubling the daily dose rate very nearly halves the survival time.[33] The dose rate of 0.05 μC/g of Ra^{223} declined exponentially from 425 rad/day on the first day to 140 rad/day on the 10th day, whereas for Ra^{226} the dose rate remained essentially constant for the first 10 days at a level of 275 rad/day for an injection of 0.172 μC/g. This difference in radiation dose rate only partially accounts for the eightfold difference between our calculated LD_{50}/30 days for Ra^{226} and that which has been observed by other workers.

There is one striking difference between the status of our Ra^{223} rats and those injected with natural radium by other investigators. Casarett[34] and Murray[35] found large active centers of myelopoiesis of all types in the spleens of both rats and mice within 20 days (and occasionally as early as 10 days) after Ra^{226} injections below the observed acutely lethal level. The bone marrow at these Ra^{226} dosages was aplastic except for small cores of cellular marrow deep in the central shafts of the long bones. In our Ra^{223}-injected animals with bone marrow hypoplasis comparable to that produced by nearly lethal amounts of natural radium, only minimal ectopic myelopoiesis was found in either spleen or liver except for the very longest-term survivors at the lowest Ra^{223} level. Jacobsen et al. attribute the survival of mice given large amounts of the bone-seeking radioisotopes of the alkaline earths to the

rapid development and persistence of ectopic erythropoiesis in the spleen.[11] They found that splenectomized mice developed a much more profound anemia after injection of Sr^{89} than did intact mice whose spleens became actively myelocytic as early as 3 days after the Sr^{89} injection. For some reason, as yet unknown, our Ra^{223}-injected animals were unable to respond to the stimulus of massive marrow destruction by the rapid initiation of ectopic splenic myelopiesis. The difference in the capacity for myelopoietic response by the spleens of the animals we used and those employed by other investigators may finally reconcile the previously reported toxicity of natural radium, Ra^{226}, with the toxic dosage we calculated from experiments with the Ra^{223} isotope.

APPENDIX: CALCULATION OF RADIATION DOSE TO THE SKELETON AND BONE MARROW

Loevinger, Holt, and Hine[36] give the following equations for the dose rate and integral dose delivered by internally deposited radioisotopes:

$$\text{Dose rate (rad/day)} = 51.2\ E\ C_t, \text{ and} \tag{A1}$$

$$\text{Integral dose (rad)} = 51.2\ E \int_0^t C_t dt, \tag{A2}$$

where the rad is 100 ergs absorbed per gram of tissue, E is the average energy expressed in Mev, C_t is the concentration of the isotope in the tissue, expressed in microcuries per gram, and t is the time after injection, in days.

The average energy of Ra^{223} in equilibrium with its daughters is

$$E_{223} = 26.3 + 2.65/3 = 27.2 \text{ Mev.}^2 \tag{A3}$$

The half lives of the Ra^{223} daughters are short, and radioactive equilibrium is established within 3 hours after separation of Ra^{223} from Ac^{227}. The half life of the radon daughter Rn^{219} is only 3.9 sec, and its escape from the site of deposition of the parent Ra^{223} can be neglected.

The mean skeletal weight of the rats used in these experiments was 27 g. For the sake of simplicity it was assumed that the Ra^{223} was uniformly distributed throughout the skeleton. Autoradiographic studies by Arnold, among others, show that about half the retained radium is deposited on bony surfaces in regions of new bone formation or remodeling, and the remainder is fairly evenly dispersed throughout the compact bone.[37] The following equations obtained from Fig. 33 were used to calculate C_t for the various dosage levels of Ra^{223}:

0.004 μC/g, at the lowest dosage level,

$$C_t = 0.74\ e^{-0.338t} + 1.52\ e^{-0.009t}, \tag{A4}$$

and, at the higher dosage levels,

$$C_t = 0.99\ e^{-0.338t} + 1.63\ e^{-0.004t}. \tag{A5}$$

Substituting the appropriate expression for C_t in Eq. (A1) and including the necessary correction for radioactive decay of the 11.2-day Ra^{223} ($\lambda = 0.062\ \text{day}^{-1}$), one finds the dose rate in the skeleton is

$$\text{rad/day} = 14\ D\ (0.74\ e^{-0.4t} + 1.52\ e^{-0.071t}), \tag{A6}$$

where D is the Ra^{223} dosage in microcuries.

The accumulated dose at any subsequent time after injection of 1 μC of Ra^{223} is obtained by integration of Eq. (A6):

$$\text{rad} = 14\ \left[1.85\ (1 - e^{-0.4t}) + 21.4\ (1 - e^{-0.071t})\right]. \tag{A7}$$

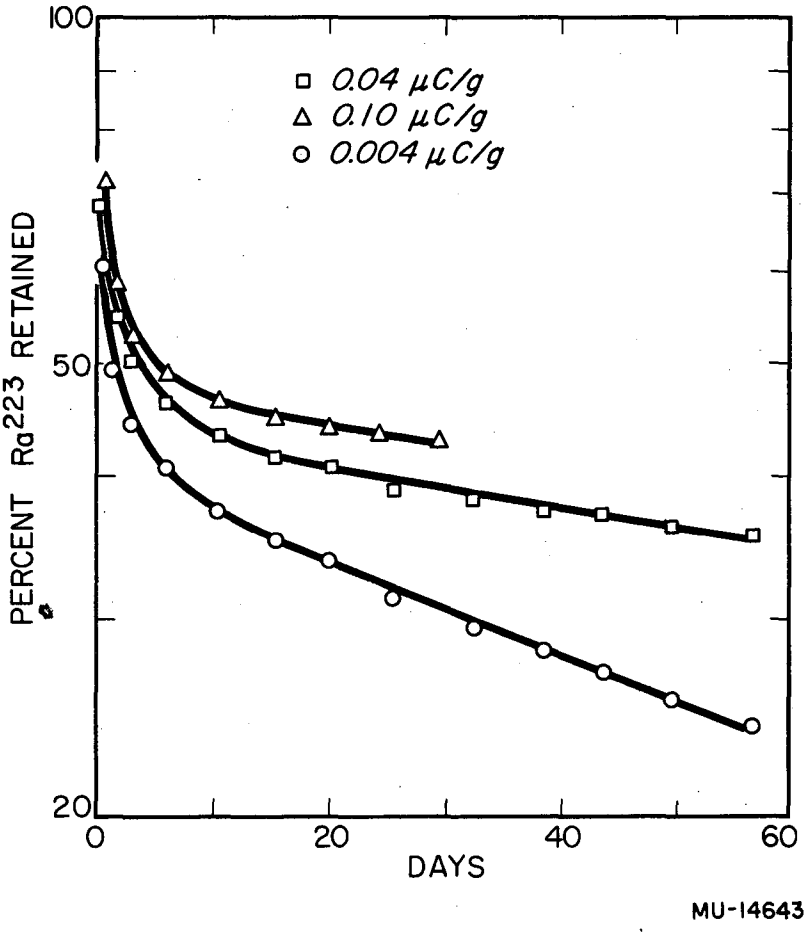

Fig. 33. Retention of various dosage levels of Ra^{223} as a function of time after injection.

The equations for dose rate and integral dose at higher injection levels were calculated in a similar fashion by use of C_t from Eq. (A5).

It was also of interest to compare the dosage for Ra^{223} with that for natural radium, Ra^{226}, primarily because of the use of Ra^{226} as the standard for evaluating biological hazard,[38] also because of the effect of rate of energy absorption on biological response.

The most extensive studies of the metabolism and toxicity of Ra^{226} in small animals have been made by Norris and Evans[5] and by the Rochester group.[4] These investigators used freshly purified preparations of Ra^{226} (less than 6 months old) in order to avoid the side effects of RaD, an isotope of polonium. In addition, Norris and Evans aerated their radium solutions prior to injection, thus removing essentially all the radon and its short-lived daughters and eliminating uncertainties in dosage from possible loss of radon during the injections. Therefore we have made two sets of calculations: first, for the equilibrium mixture of freshly purified radium (including the shorter-lived members of the series Rn^{222}, Po^{218}, Pb^{214}, Bi^{214}, and Po^{214}); and second, for freshly purified radium aerated prior to use. In the latter the calculations take into account the subsequent growth of radon and its daughters. In both cases a correction was introduced to account for the loss by exhalation of approximately 85% of the radon produced in vivo.[5]

The average energy per disintegration of the equilibrium mixture is
$4.78 + 0.15 \times 20.05 = 7.79$ Mev,
and, for the aerated solution,

$$E_{226\ aer} = 4.78 = 0.15 \times 20.05\ (1 - e^{-0.18\ t})\ \text{Mev.} \qquad \text{(A8)}$$

Because of the good agreement between the retention data for our high levels of Ra^{223} and the data from Norris and Evans[5] and from Silberstein[4] for Ra^{226} retention, the expression for C_t was taken from Eq. (A5). The dosage rate for the equilibrium mixture of Ra^{226} and its shorter-lived daughters was

$$\text{rad/day} = 3.98\ D\ (0.99\ e^{-0.34\ t} + 1.63\ e^{-0.004\ t}). \qquad \text{(A9)}$$

The dosage rate for Ra^{226} from which the radon daughter had been removed by aeration was, from Eqs. (A5) and (A8),

$$\text{rad/day}_{aer} = 2.45\ D + 1.54\ D(1 - e^{-0.182\ t})\ (0.99\ e^{-0.34\ t} + 1.63\ e^{-0.004\ t}) \qquad \text{(A10)}$$

The dosage rates of 1 μC of Ra^{223} and 1 μC of Ra^{226}, both equilibrium mixture and aerated, are shown in Fig. 34 for a 250-g rat with a 27-g skeleton. The intergral doses for the various levels of administration of Ra^{223} and for 1μC of Ra^{226} are shown in Table A-I for several postinjection intervals.

In estimating the radiation dosage to the bone marrow one must consider (a) dissipation of energy in the bone itself, a function of the random orientation of the emitted particles; (b) deposition of the isotope in regions of bone remote from the surfaces of the marrow cavities; and (c) the geometrical configuration of the marrow cavities, particularly for alpha emitters whose

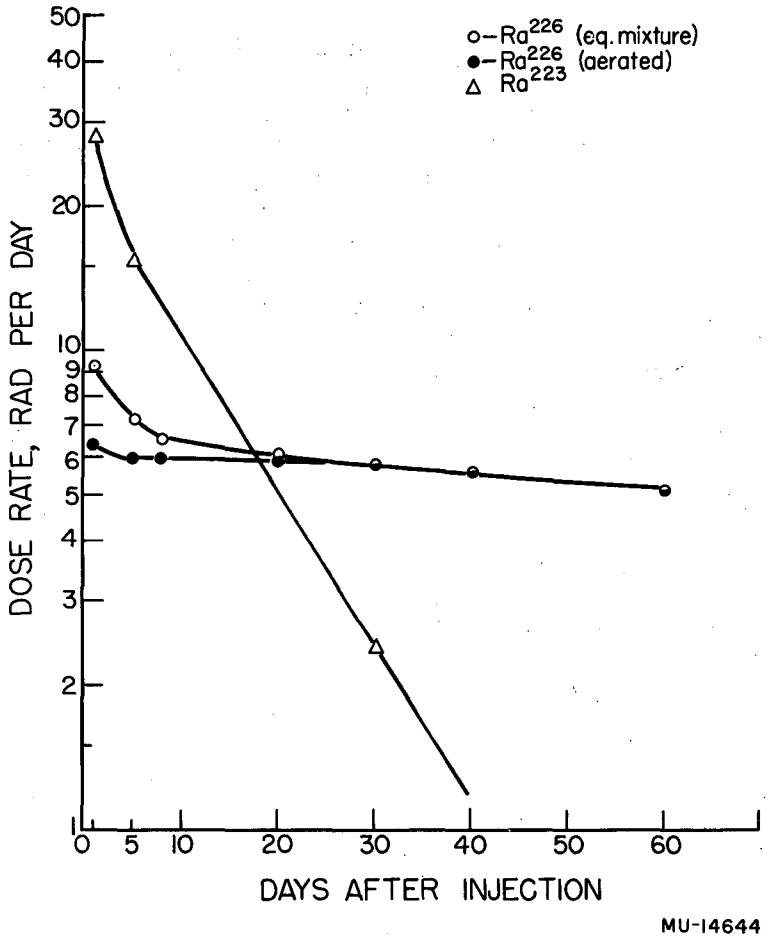

Fig. 34. Comparison of the change in daily dose rates from internally deposited Ra^{226} and Ra^{223} as functions of time after injection.

Table A-I

Estimated accumulated radiation dose to the rat skeleton[a] following administration of radium isotopes, assuming uniform skeletal distribution of radium

	Accumulated skeletal dose (rad)						
	Ra^{223}					Ra^{226}	
Dosage, μC/rat	1	5	10	17.5	25	1(eq. mix)	1(aerated)
μC/g	0.004	0.02	0.04	0.07	0.10	0.004	0.004
Days after injection							
1	28	140	338	590	845	10	6.4
5	108	565	1210	2120	3150	42	31
30	280	1380	3200	5600	8050	193	179
60	295	1540	3600	-	-	351	341
112	300	1560	3680	-	-	593	583

[a]Dose to marrow and to epipyseal plate calculated at 1.54 times the uniform skeletal dose. See text.

particle range is no more than 100 microns. If comparisons are limited to groups of animals of the same species and of a specific strain, age, and sex, the geometrical factor (c) should not seriously bias the data.

It was assumed that 50% of the energy available from radioisotopes that are deposited on bony surfaces is absorbed in the bone itself and does not affect the marrow directly. It was also assumed that about 50% of retained radium is distributed in compact bone at distances from the marrow cavities greater than the range of the alpha particles.

An estimate of the volume of marrow was obtained from several sources. Finch found that erythroid cells of the marrow of dogs and rabbits constitutes 0.9% of the body weight.[39] Garcia has calculated the mass of erythropoietic marrow as 0.8% of the body weight, from radioiron studies in young adult male rats.[40] From the average of the above values and a ratio of erythrocytic to granulocytic cells of 1.17 ± 0.11 for young adult female Sprague-Dawley rats, the total mass of functional marrow is 1.58% of the body weight. This calculated value agrees with the value obtained experimentally by Yoffey for the total marrow mass of the adult male guinea pig, 1.75%.[10] Yoffey's figure also takes into account the fat content of the marrow.

From Yoffey's data the marrow mass of a 250-g rat was calculated as 4.38 g. The marrow dose is then

$$\text{Marrow dose (in rad)} = \frac{27\text{g}}{4.38\text{g}} \times 0.25 \times \text{skeletal dose} = 1.54 \times \text{skeletal dose (in rad)}. \quad \text{(A11)}$$

Equation (A11) assumes that the marrow is uniformly irradiated. Histological evidence in this paper and others[37,41] shows that this is an oversimplification. The error introduced should not be too large for small animals such as mice with small marrow cavities. The data on red cell Fe^{59} uptake in these experiments indicates that for the rat the marrow dose calculated by use of the above assumptions may be in error by as much as a factor of 3.3, inasmuch as direct irradiation accounted for destruction of only 30% of the total marrow mass.

The radiation dose to the epiphyseal cartilage in adult female rats was assumed to be the same as that calculated for the marrow. The mean plate width in the animals used for these experiments was 70 ± 4.9 microns, which is approximately the same as the alpha-particle range.

BIBLIOGRAPHY

1. Campbell, Robajdek, and Anthony, The Metabolism of Ac^{227} and Its Daughters Th^{227} and Ra^{223} By Rats, Radiation Research 4, 294-302 (1956).

2. Hollander, Perlman, and Seaborg, Table of Isotopes, Revs. Modern Phys. 25, 469-651 (1953).

3. T.G. Hennessey, and R.L. Huff, Depression of Tracer Iron Uptake Curve in Rat Erythrocytes Following Total Body x-Irradiation, Proc. Soc. Exptl. Biol. Med. 73, 436-439 (1950).

4. H.E. Silberstein, Radium Distribution and Excretion Studies with Rats, in Biological Studies with Polonium, Radium and Plutonium, R.M. Fink, Ed. (McGraw-Hill, New York, 1950), Ch. 6 (This book will be referred to hereafter as NNES VI-3).

5. W.P. Norris, and H.P. Evans, Studies of the Metabolism and Toxic Action of Injected Radium, Univ. Chicago Metallurgical Lab., CH-3852 March 1948)

6. Storer, Harris, Furchner, and Langham, The Relative Biological Effectiveness of Various Ionizing Radiations in Mammalian Systems, Radiation Research 6, 188-288 (1957).

7. R.A. Conard, Some Effects of Ionizing Radiation on the Physiology of the Gastrointestinal Tract: a Review, Radiation Research 5, 167-188 (1956).

8. W.A.D. Anderson, Pathology (Mosby, St. Louis, 1948), pp. 76-77.

9. T.G. Hennessey and J.P. O'Kunewick, Radioiron Study of Erythropoiesis After x-Irradiation, UCLA-383, Dec. 1956.

10. J.M. Yoffey, The Mobilization and Turnover Times of Cell Populations in Blood and Blood-Forming Tissues, J. Histochem. Cytochem. 4, 516-530 (1956).

11. Jacobson, Simmons, and Block, The Effect of Splenectomy on the Toxicity of Sr^{89} to the Hematopoietic System of Mice J. Lab. Clin. Med. 34, 1640-1655 (1949).

12. Boyd, Silberstein, Fink, and Frankel, et al., Pilot Studies on the Intravenous Lethal Dosage of Polonium, Plutonium, and Radium in Rats NNES VI-3, Ch. 7.

13. Durbin, Jeung, Williams, Parrott, and Hamilton, Relationships Between Radiation Damage and Endocrine Deficiency After Massive Doses of Iodine-131 in Rats, Radiation Research 7, 313 (1957). Abstract.

14. T.F. Dougherty, and A. White, Influence of Hormones on Lymphoid Tissue Structure and Function, the Role of Pituitary Adrenotrophic Hormone in the Regulation of the Lymphocytes and Other Cellular Elements of the Blood, Endocrinology 35, 1-14 (1944).

15. C.K. Drinker, and J.M. Yoffey, Lymphatics, Lymph and Lymphoid Tissue (Harvard University Press, Cambridge, 1941), p. 197.

16. C.H. Best, and N.B. Taylor, The Physiological Basis of Medical Practice Fourth Edition (Williams and Wilkins, Baltimore, 1945) pp. 70-76.

17. O.A. Trowell, The Sensitivity of Lymphocytes to Ionizing Radiation, J. Path. Bact. 64, 687-704 (1952).

18. Berlin, Meyer, and Lazarus, Life Span of the Rat Red Blood Cell as Determined By Glycine-2-C^{14}, Am. J. Physiol. 165, 565-567 (1951).

19. Berlin, Huff, and Hennessey, Iron Metabolism in the Cobalt-Polycythemic Rat, J. Biol. Chem. 188, 445-450 (1951).

20. Asling, Durbin, Johnston, and Hamilton, The Effect of Propyl Thiouracil on the Recovery of Rat Thyroid Gland from Irradiation with Astatine-211. Anat. Record (in press).

21. M. Heller, Histopathology of Irradiation from External and Internal Sources, NNES IV-22.

22. Becks, Simpson, and Evans, Ossification at the Proximal Tibial Epiphysis in the Rat. I. Changes in the Female Rat with Increasing Age. Ant. Rec. 92, 109-119 (1945).

23. Owen, Sissons, and Vaughan, The Effect of a Single Injection of High Dose of Sr^{90} (500-1000 μC/kg) in Rabbits, Brit. J. Cancer 11, 229-248 (1957).

24. P.W. Durbin and H. Jones, Estimation of the Turnover Equation of Strontium-90 for Human Bones (Abstract) UCRL-8083, Dec. 1957.

25. W.B. Looney, Late Effects (Twenty-Five to Forty Years) of the Early Medical and Industrial Use of Radioactive Materials. Part I, J. Bone Joint Surg. 37-A, 1169-1187 (1955).

26. J.P. Weinmann, and H. Sicher, Bone and Bones (Mosby St. Louis, 1947), pp 51-53.

27. A.A. Maximow, and W. Bloom, A Textbook of Histology 4th Ed (Saunders, Philadelphia, 1942), p. 148.

28. R. de Marneffe, Recherches Morphologiques et Experimentales sur la vascularisation osseuse. Les Editions "Acta Medica Belgica", Bruxelles, 1951.

29. R.P. Rhoades, The Vascular System, in Histopathology of Irradiation, NNES IV-22I, Ch. 16.

30. M.A. Bloom, Bone Marrow in Histopathology of Irradiation NNES IV-22I, Ch. 6.

31. G.A. Boyd, and R.M. Fink, Simultaneous Studies on the Intravenous Lethal Dosage of Polonium, Plutonium and Radium in Rats, NNES VI-3, p. 333.

32. Murray, Tyree, Ismond, and Svihla, Materials and Methods in, Histopathology of Irradiation, NNES IV-221, p. 14.

33. Grahn, Sacher, and Hamilton, Progress Report: Gamma-Ray Toxicity Program. Genetic Variation in the Survival Time of Mice Under Daily Exposure to Co^{60} Radiation. I. in Quarterly Report of the Biological and Medical Research Division, (Argonne National Laboratory), ANL-5597, pp. 36-38 (1956).

34. Casarett, Metcalf, and Boyd, Pathology Studies on Rats Injected with Polonium, Plutonium, and Radium, NNES VI-3, pp. 343-389.

35. R.G. Murray, The Spleen in Histopathology of Irradiation NNES IV-22I, pp. 273-283.

36. Loevinger, Holt, and Hine, Internally Administered Radioisotopes, in Radiation Dosimetry J.G. Hine, and G.L. Brownell, Eds (Academic New York, 1956), pp. 801-873.

37. J.S. Arnold, General Features of Bone Deposition in Second Annual Conference on Plutonium, Radium, and Mesothorium, Radiobiology Laboratory, Univ. Utah, College of Medicine, Salt Lake City, June 1954, pp. 112-129.

38. National Bureau of Standards, Maximum Permissible Amounts of Radioisotopes in the Human Body and Maximum Permissible Concentrations in Air and Water U.S. Dept. Commerce, Handbook 52, March 1953.

39. Finch, Donohue, Reiff, and Hanson, Quantitative Aspects of Erythropoiesis, Fed. Proc. 16, 38 (1957). Abstract.

40. J.F. Garcia, Studies on Erythropoiesis as a Function of Age in the Normal Male Rat, UCRL-3516, Sept. 1956.

41. J.M. Vaughan, The Effects of Radiation on Bone in Biochemistry and Physiology of Bone, G.H. Bourne, Ed. (Academic Press New York, 1956), pp. 729-765.